5-2009

Anti-islanding schemes for machine-based distributed generation

Temesgen Tadegegn
University of Nevada, Las Vegas

ANTI-ISLANDING SCHEMES FOR MACHINE-BASED DISTRIBUTED GENERATION

by

Temesgen B. Tadegegn

Associate Degree in Business Administration
Ethiopian Adventist College
1996

Bachelor of Technology
Defense University of Ethiopia
2002

A thesis submitted in partial fulfillment
of the requirements for the

Master of Science Degree in Electrical Engineering
Department of Electrical and Computer Engineering
Howard R. Hughes College of Engineering

Graduate College
University of Nevada, Las Vegas
May 2009

UNLV
UNIVERSITY OF NEVADA LAS VEGAS

Thesis Approval

The Graduate College
University of Nevada, Las Vegas

April 16 , 2009

The Thesis prepared by

Temesgen Tadegegn

Entitled

Anti-islanding Schemes for

Machine-based Distributed Generation

is approved in partial fulfillment of the requirements for the degree of

Master of Science in Electrical engineering

[redacted]
Examination Committee Chair

[redacted]
Dean of the Graduate College

[redacted]
Examination Committee Member

[redacted]
Examination Committee Member

[redacted]
Graduate College Faculty Representative

ABSTRACT

Anti-islanding Schemes for Machine-Based Distributed Generation

by

Temesgen Tadegegn

Dr. Yahia Bahgzouz, Examination Committee Chair
Professor of Computer and Electrical Engineering
University of Nevada, Las Vegas

The most common method of detecting the islanding in a machine-based distributed generator (DG) is to establish an under/over frequency and under/over voltage window within which a synchronous DG is allowed to operate. When such a DG is islanded from the utility system, the frequency or voltage will quickly move outside the operating window if there is a sufficient difference between the local load and DG power generation level. However, there is a possibility that the system voltage and frequency will be maintained within the specified limits following loss of the grid in cases where the load and generator are matched. Therefore, special means are required to detect the loss of the grid in this particular situation.

This thesis investigates effective ways to detect islanding of machine-based DG unit when there is a match between generation and demand in the islanded section of the distribution system. A combination of both passive and active techniques will be considered in the analysis. Typical passive techniques are based on the rate of change of frequency, output power, voltage, power factor, voltage unbalance, or voltage total

harmonic distortion. On the other hand, active schemes detect the islanding by directly interacting with the utility system. Three active methods that were recently proposed include the following: (A) Reactive error export detection (which controls the embedded generator excitation current so that it generates a known value of reactive current, which cannot be supported unless the generator is connected to the grid). (B) Fault level monitoring (which makes detection possible in half a cycle by using point-on-wave thyristor switching triggered near the voltage zero point). (C) Positive feedback (that results in unstable frequency or voltage once the DG is islanded). The analysis will be illustrated through computer simulations.

TABLE OF CONTENTS

LIST OF FIGURES

LIST OF SYMBOLS

- δ: power angle of the generator
- H: inertia constant of the generator
- i_d: armature d axis terminal current
- i_q: armature q axis terminal current
- i_{fd}: field winding terminal current (reflected to the stator)
- i_{ld}: d axis damper winding current (reflected to the stator)
- i_{lq}: q axis damper winding current (reflected to the stator)
- L_l: stator winding inductance of the generator
- L_{ld}: d axis leakage inductance of the generator
- L_{lq}: q axis leakage inductance of the generator
- L_{ad}: d axis magnetizing inductance of the generator
- L_{aq}: q axis magnetizing inductance of the generator
- L_{fd}: field leakage inductance of the generator
- L_{md}: d axis coupling inductance
- R_a: stator-winding resistance of the generator
- T_m: mechanical torque of generator
- T_e: electromagnetic torque of the generator
- u_d: armature d axis terminal voltage
- u_q: armature q axis terminal voltage

- u_{fd}: field winding terminal voltage (reflected to the stator)
- ω_r: rotating speed of the generator
- ψ_d: total armature flux in d axis
- ψ_q: total armature flux in q axis
- Ψ_{fd}: field winding flux linkage of the generator
- Ψ_{1d}: d axis damper winding flux linkage of the generator
- Ψ_{1q}: q axis damper winding flux linkage of the generator

ABBREVIATIONS

- AI: anti-islanding
- DG: distributed generation
- NDZ: non-detection zone
- p_f: power factor
- Q_f: quality factor

CHAPTER 1

INTRODUCTION

Traditionally, distribution power systems are configured in radial structures. Power and short-circuit currents flow uni-directionally from distribution substations. Most protection, monitoring, and control devices are designed based on this configuration. Recently, DG has begun to emerge in the energy market because of its value for such things as peak shaving, combined heat and power, renewable portfolios, and transmission and distribution infrastructure deferral. These and other uses provide economical and environmental incentives to promote distributed generation. However, due to the historical distribution infrastructure and the energy market structure there are regulatory and technical barriers to DG entering the current energy market.

One important requirement for distributed generators is anti-islanding capability. It is the capability of a distributed generator to detect if it operates in an islanded system and to disconnect itself from the system in a timely fashion. Islanding occurs when a portion of the distribution system becomes electrically isolated from the remainder of the power system, yet continues to be energized by distributed generators. The incapability to trip islanded generators can lead to many problems for the generator and the connected loads. The existing practice is to disconnect all distributed generators immediately after islanding. The purpose of this chapter is to provide background information on the

operation of power distribution systems and to elaborate the importance of anti-islanding protection.

1.1 Distributed Generator Islanding

A sample distribution system is shown in Figure 1.1. The substation transformer steps down the transmission voltage into the distribution voltage and is connected to several distribution feeders. One of the feeders is shown in detail. There are many load connection points along the feeder. Large distributed generators are typically connected to the primary feeders, DG1 and DG2. These are mainly synchronous generators. Inverter based PV systems are connected to the low voltage secondary feeders, DG3, since they are considered as small distributed generators.

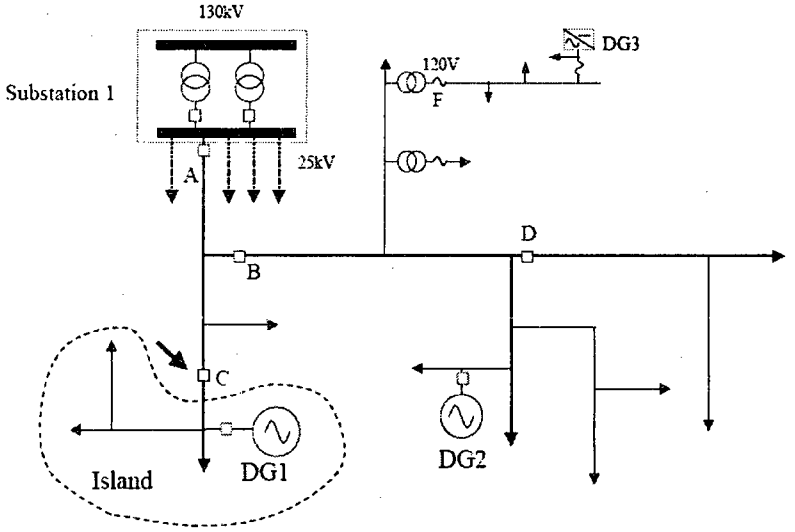

Figure 1.1 Typical distribution system with distributed generators.

Islanding happens when circuit breaker C opens and DG1 feeds the resultant island. It could also happen when the fuse at point F melts and DG3 feeds the resultant island. In this case, the DG will feed the local loads, forming a small-islanded power system. The island is an unregulated electrical system with unpredictable behavior due to the power mismatch between the load and generation and the inability to control voltage and frequency. The problems associated with such islanded systems are as follows:

1. Since the utility is no longer controlling the voltage and frequency, voltage and frequency can vary significantly. If the distributed generators do not provide regulation of voltage and frequency, there is a probability of damage to customer equipment.
2. Islanding may be dangerous for utility line-workers or the public since it leaves a line to remain energized that may be considered disconnected.
3. It is unsafe when a distributed generator is reconnected to the supply system after islanding. Since the generators will not be in synchronism with the system at the instant of reconnection. Such out-of-phase operation of a circuit breaker can cause a large current flow to the generators resulting in re-tripping of the supply system.
4. Islanding may interfere with the manual or automatic restoration of service to customers.

The current industry practice is to disconnect all DGs immediately so that the entire feeder becomes de-energized [1, 2]. This helps to avoid equipment damage and eliminates safety hazards. To effectively disconnect all DGs when Islanding occurs, each

DG must have the capability to detect islanding conditions and to stop feeding the local loads.

1.2 Detection of Islanded Power Systems

As soon as an island is formed, it should be detected immediately in order to satisfy the conditions stated above. The basic requirements for a successful detection are:

1. The scheme must detect any possible formations of islands. Since every islanding can have different mixture of loads and distributed generators, the nature of each island can be quite different. A reliable anti-islanding scheme must be able to avoid all possible islanding conditions.
2. The scheme should detect islanding conditions within the required time frame as specified in IEEE regulations. A circuit breaker is typically programmed to reenergize its downstream system after about 0.5 to 1 second delay. Ideally, the anti-islanding scheme must trip its DG before the reclosing takes place.

Many anti-islanding techniques have been proposed and a number of them have been implemented in actual DG projects [3] or incorporated into the controls of inverters used in utility-interactive DG applications. When designing an anti-islanding scheme, it is crucial to assess the characteristics of the distributed generators. Distributed generators may be grouped into the following three categories:

1. **Synchronous generator**: This type of Distributed Generator is typically connected to the primary feeder with a size as high as 30MW. Synchronous generators are highly capable of sustaining an island. Anti-islanding protection for

synchronous generators is very difficult due to its large power rating and it has been a major research topic.

2. **Induction generator**: This type of Distributed Generator is typically connected to the primary feeder as well with a size in the range of 10 to 20 MW. Anti-islanding protection is not quite an issue for induction generators. They are not capable of sustaining an island due to their demand for reactive power supply from main Grid. Hence, anti-islanding protection is such a problem for induction generators.
3. **Inverter-based generator**: This type of Distributed Generator has relatively a small size in the range of a few hundred watts to few hundred kW and is commonly connected to the secondary feeder. These generators can be photovoltaic panels, fuel cells, micro-turbines etc. Since it is the inverter that interacts with the supply system, all inverter-based DGs have operating characteristics with respect to grid interaction primarily determined by the inverter topology and controls. The inverter-based DGs are capable of sustaining an island; however, the utility-interactive inverters can be designed to detect and control islanding conditions. As a result, many inverter specific anti-islanding techniques have been proposed.

These techniques can be broadly classified into two types according to their working principles [3]. This classification is shown in Figure 1.2. The first type consists of communication-based schemes and the second type consists of local detection schemes. The communication-based schemes use telecommunication means to alert and trip DGs when islands are formed. Their performance is independent of the type of

distributed generators involved. The second type is local detection schemes that rely on the voltage and current signals available at the DG site. An islanding condition is detected if indices derived from the signals exceed certain thresholds. A representative example is the frequency relay.

The local detection schemes can be further divided into two sub-types. One is the passive detection method, which makes decisions based on measured voltage and current signals only. Another type is the active detection method. Such methods inject disturbances into the supply system and detect islanding conditions based on system responses measured locally. The active method is widely used by inverter-based DGs due to its ease of implementation on such systems. Although some of the local detection schemes can be applied to both types of DGs, their performances can differ, as they are dependent on the operating characteristics of the DGs involved.

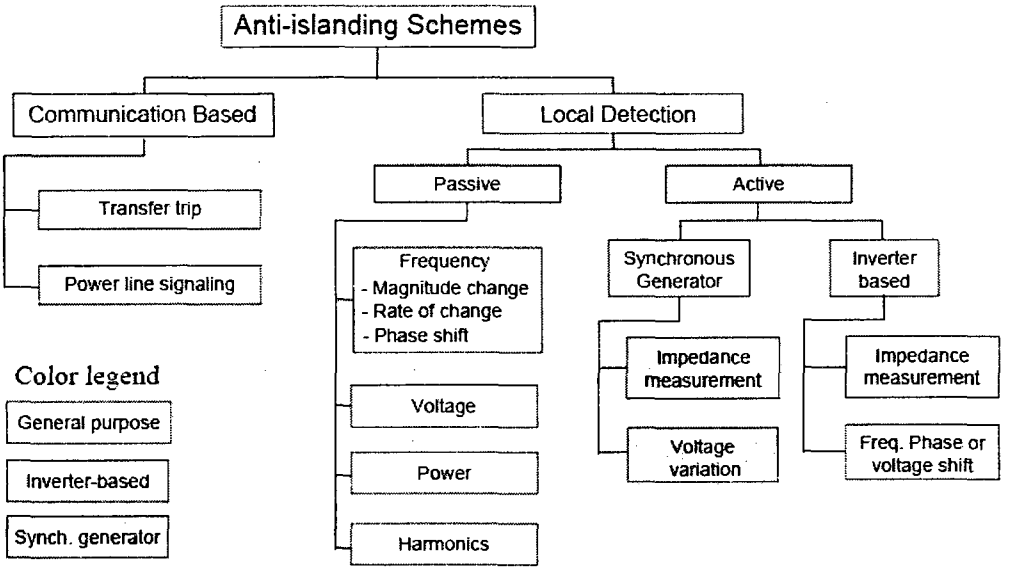

Fig. 1.2 Classification of anti-islanding schemes

In this thesis, an alternative method using positive feedback is presented and tested using computer simulations. The study is done only on synchronous generators connected to an infinite bus with intermediate static loads like resistors, capacitors and inductors, dynamic loads and also induction motor. We focus on synchronous generator because anti-islanding protection for synchronous generators has emerged as the most challenging task faced by the DG industry and also it is not a major issue in Induction generators.

The content of this thesis is as follows: chapter 2 covers the synchronous generator dynamic modeling, chapter 3 discusses about non-detection zones, chapter 4 explains positive feedback anti-islanding schemes with simulations and finally chapter 5 gives the outcomes of this study.

CHAPTER 2

SYNCHRONOUS GENERATOR MODELING

The purpose of this chapter is to introduce a synchronous generator dynamic model that takes into account all relevant dynamic phenomena occurring in the machine. Since this model has been widely known [12], only the main assumptions and results will be presented.

2.1 Assumptions for Model Development

A three-phase, wound-field synchronous generator has three identical armature windings symmetrically distributed around the air-gap, and one field winding. One or more damper windings can also be present and, for convenience in this section, it is assumed that one damper winding is present in each machine's axis. Normally, armature windings are placed on the stator, and field and damper windings on the rotor. However, there are cases, when armature windings are placed on the rotor and field winding on the stator (the exciter has no damper windings). This does not affect the machine modeling approach at all, since only relative motion between the stator and rotor windings is important. Therefore, throughout this paper, the rotor windings will always imply the field winding (and damper winding, if existent) placed at the opposite side of the air gap with respect to the three-phase armature windings.

2.2 Development of the Model Equations and Equivalent Circuit

A synchronous machine can be described by a system of n+ 1 equation, n of which are electrical and one of which is mechanical. The number n of electrical equations is equal to the number of independent electrical variables necessary to describe the machine. These variables can be either currents or flux linkages. Currents are chosen to be the independent variables in this thesis. Electrical equations are obtained by writing Kirchoff's voltage law for every winding, i.e. by equating the voltage at the winding's terminal to the sum of resistive and inductive voltage drops across the winding [4], [5]. Note that damper windings, if present, are always short-circuited. Therefore, their terminal voltage is equal to zero.

In order to correctly calculate the inductive voltage drop across a winding, the total magnetic flux linked with the winding needs to be evaluated. This is achieved by means of an inductance matrix, which relates to all winding flux linkages to all winding currents. When that is done for a salient-pole synchronous machine, an inductance matrix dependent on the rotor position is obtained. This dependence is due to the magnetic asymmetry of the rotor: because of the way the rotor of a salient pole machine is shaped, there exists a preferable magnetic direction. This direction coincides with the direction of the flux produced by the field winding, and is defined as machine's d axis. The machine's q axis is placed at 90 electrical degrees (in a counterclockwise direction) with respect to the machine's d axis. Then, the rotor position can be expressed by means of an angle, named θ, between the magnetic axis of the armature's phase a and the rotor's q axis.

Dependence of the inductance matrix on the rotor position represents the main difficulty in modeling the synchronous machine. A solution to this problem is to change

the reference system, or frame, in which the machine's electrical and magnetic variables are expressed. So far, the reference frame intuitively used was the so-called stationary, or stator, or abc reference frame. In it, variables are expressed as they can actually be measured in the machine, but the machine parameters are time variant (since θ is a function of time). It can be shown that the only reference frame that provides constant machine parameters is the rotor, or dq, reference frame [12]. In it, all variables are expressed in a form in which a hypothetical observer placed on the rotor would measure them. The following transformation matrix gives transformation from the abc to the dq reference frame:

$$T = \sqrt{\frac{2}{3}}\begin{bmatrix} \sin\theta & \sin\left(\theta-\frac{2\pi}{3}\right) & \sin\left(\theta+\frac{2\pi}{3}\right) \\ \cos\theta & \cos\left(\theta-\frac{2\pi}{3}\right) & \cos\left(\theta+\frac{2\pi}{3}\right) \end{bmatrix} \qquad 2.1$$

Inverse transformation (from the dq to the abc reference frame) is then given by

$$Tinv = \begin{bmatrix} \sin\theta & \cos\theta \\ \sin\left(\theta-\frac{2\pi}{3}\right) & \cos\left(\theta-\frac{2\pi}{3}\right) \\ \sin\left(\theta+\frac{2\pi}{3}\right) & \cos\left(\theta+\frac{2\pi}{3}\right) \end{bmatrix} \qquad 2.2$$

In (2.1) and (2.2), θ is calculated as

$$\theta(t) = \int \omega(\xi)\, d\xi + \theta o \qquad 2.3$$

where ω represents the rotor's (electrical) speed.

Therefore, any set of three-phase variables f_a, f_b and f_c expressed in the abc reference frame can be transformed in dq reference frame variables f_d and f_q by multiplying them by:

$$\begin{bmatrix} fd \\ fq \end{bmatrix} = T \begin{bmatrix} fa \\ fb \\ fc \end{bmatrix} \tag{2.4}$$

and vice versa:

$$\begin{bmatrix} fa \\ fb \\ fc \end{bmatrix} = Tinv \begin{bmatrix} fd \\ fq \end{bmatrix} \tag{2.5}$$

Note that transformation of the variables, as defined by (2.1) and (2.2), preserves total system power: in every time instant, power in the abc reference frame is equal to the power in the dq reference frame.

When the machine's electrical equations are transformed from the abc to the dq reference frame with magnetic saturation and magnetic hysteresis neglected and the air gap flux considered to be sinusoidally distributed along the air gap, they assume the following form [12]:

- Voltage equations

$$v_d = p\Psi_d - \Psi_q - R_a i_d \tag{2.6}$$

$$v_q = p\Psi_q + \Psi_d \omega_r - R_a i_q \tag{2.7}$$

$$e_{fd} = p\psi_{fd} + R_{fd} i_{fd} \tag{2.8}$$

$$0 = p\psi_{1q} + R_{1d} i_{1d} \tag{2.9}$$

$$0 = p\psi_{1d} + R_{1d} i_{1d} \tag{2.10}$$

- Flux equation

$$\Psi_d = -(L_{ad} + L_l) i_d + L_{ad} I_{fd} + L_{ad} i_{1d} \tag{2.11}$$

$$\Psi_q = -(L_{aq} + L_l) i_q + L_{aq} i_{1q} \tag{2.12}$$

$$\Psi_{fd} = (L_{ad} + L_{fd}) i_{fd} + L_{ad} i_{1d} - L_{ad} i_d \tag{2.13}$$

$$\Psi_{1d}=L_{ad}i_{fd}+(L_{1d}+L_{ad}i_{fd})i_{1d}-L_{ad}i_d \quad 2.14$$

$$\Psi_{1q}=(L_{1q}+L_{aq})i_{1q}-L_{aq}i_q \quad 2.15$$

- Air-gap torque equation

$$T_e=\psi_d i_q-\psi_q i_d \quad 2.16$$

Equations (2.6)-(2.16) describe the synchronous generator's equivalent circuit in the rotor reference frame shown in Fig. 2.1.

Several comments can be made regarding this equivalent circuit: d and q axis equivalent circuits are similar to a transformer equivalent circuit. In each of them, several windings, each characterized by some resistance and leakage inductance, are coupled through a mutual coupling inductance. The difference, compared to the transformer case, is that, while a transformer equivalent circuit is an ac circuit, here, when the generator is operating in sinusoidal steady state, all voltages, currents and flux linkages are dc.

Even though armature windings are now represented in the rotor reference frame, and there are no time-variant inductances, the fact that armature windings are magnetically coupled is taken into account by the presence of cross-coupling terms in the d and q axis's equivalent circuit's armature branch. For each axis, that term is equal to the product of rotor speed and total flux linked with the armature winding of the other axis.

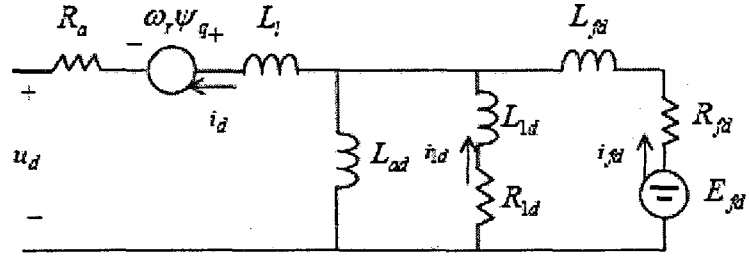

(a) d-axis equivalent circuit

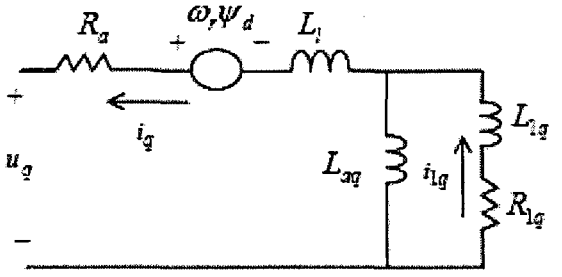

(b) q-axis equivalent circuit

Figure 2.1 Synchronous generator equivalent circuit in rotor reference frame

If a machine (such as the exciter) has no damper windings; the equivalent circuit can be easily adapted by removing the branches representing damper windings from it. The rest of the circuit remains unchanged. All rotor parameters are reflected to the armature. Therefore, when this circuit is used for simulation, and actual values of rotor variables are of interest, the turn ratio between the rotor and armature needs to be taken into account.

The above equivalent circuit describes a synchronous generator electrically. The mechanical variable is represented by the rotor speed, and the mechanical equation of the system is needed in order to complete the model. This equation relates the external torque applied to the generator's shaft to the electromagnetic torque that the machine develops internally. Generally, in case of synchronous machines, the prime mover and other essential mechanical assemblies are mounted on the same shaft. Based on the time frame involved, it is fairly a good approximation to assume the rotor mass as a rigid body. Hence for the islanding studies, the following differential equations are used to represent the synchronous machine rotor dynamics.

$$\frac{d^2\delta}{dt} = \frac{1}{2H}(Tm - Te) \quad 2.17$$

$$\frac{d\delta}{dt} = \omega r - \omega o \quad 2.18$$

where:

H is inertia constant of the generator;

T_m is mechanical torque of the generator;

T_e is electromagnetic torque of the generator;

ω_r is rotating speed of the generator.

2.3 Excitation System Model and Reactive Power Regulation

In most generators, AVRs are employed in order to supply and control the field current to supply the reactive power necessary to maintain the terminal voltage of the generator at a specified value. However, as a distributed generation, IEEE 1547 prohibits voltage regulation, unless special agreements are made. As a result the common practice for DG is reactive power (or power factor) regulation.

The exciter systems widely used by the power system industry for synchronous machines vary with the details from one manufacturer to another. But they are commonly subdivided into four different categories. A detailed explanation of modeling an excitation system for simulation studies can be found in [5]. For simplicity, the excitation system here is represented as a tuned PI controller with a necessary lag circuit. The parameters of the circuit model are given in the Appendix of this thesis. Figure 3 shows the model of the excitation system used for the machine simulation. A feedback PI controller is cascaded with the exciter to regulate the reactive power of the machine.

Therefore, when the grid is connected, the reactive power output of the machine will follow the desired reference value.

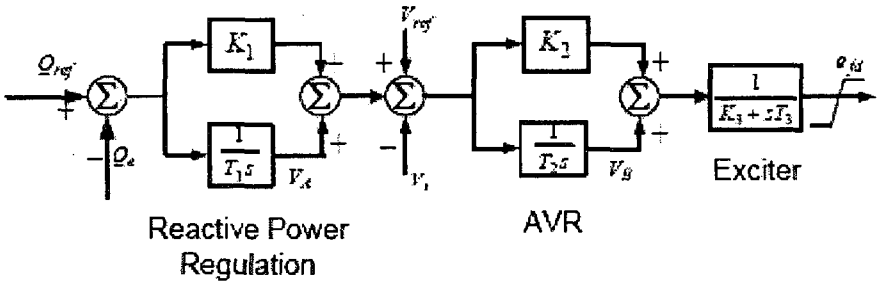

Figure 2.2 Control block diagram of excitation system

The description of the reactive power regulator and the exciter is given by[11]:

$$\dot{V}_A=(Q_{ref}-Q_e)/T_1 \qquad 2.19$$

$$\dot{V}_B=[V_{ref}-V_t+V_A+K_1(Q_{ref}-Q_e)]/T_2 \qquad 2.20$$

$$E_{fd}=[V_B-K_3e_{fd}+K_2(V_{ref}-V_t+V_A+K_1(Q_{ref}-Q_e))]/T_3 \qquad 2.21$$

where:

V_A and V_B are the intermediate variables indicated in Figure 2.2;

K_1, and K_2, K_3 are constants in the controller;

T_1, and T_2, T_3 are time constants in the controller;

Q_{ref} is the reference value of the reactive power;

Q_e is the reactive power output of the generator;

V_{ref} is the reference for the terminal voltage;

V_t is the terminal voltage of the generator;

E_{fd} is the field voltage as the input to the generator.

2.4 Governor Model and Active Power Regulation

The Governor system used in this thesis is a simplified model designed solely for power system analysis. It consists of a prime mover and provides the necessary mechanical power required by the generator. The governor is represented by a droop, which is the percentage change in speed to move the valves from fully open to fully closed, with input and the prime mover is described by a lag function. Figure 2.3 shows the typical representation of a governor and the real power regulation [12].

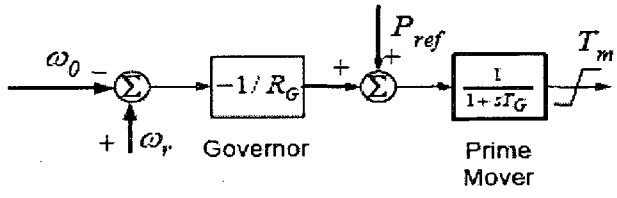

Figure 2.3 Control block diagram of governor

The governor dynamics is (including the prime mover)

$$Tm = \frac{1}{TG}\left(\Pr ef + \left(\frac{\omega r - \omega o}{RG}\right) - Tm\right) \qquad 2.22$$

where:

T_G is the time constant of the prime mover of the generator;

R_G is the governor droop.

2.5 RLC and Induction Motor Load Model

Load characteristics have an important influence on the dynamical behavior of the generator when it is islanded. The modeling of actual loads is complicated because a

typical load bus is composed of a large number of devices, such as fluorescent and incandescent lamps, refrigerators, heaters, compressors, motors, furnaces, and so on. Based on a considerable amount of simplification, two types of loads are most often investigated in the islanding studies: a RLC load and an induction motor load.

The RLC load is as simple as the aggregation of a resistor, an inductor and a capacitor in parallel. While such a load can represent the steady-state fundamental frequency characteristics of an actual load, this type of model is not a realistic representation of a load because the dynamic and non-fundamental characteristics of actual loads are not accurately simulated. Given the terminal voltage, the current through the resistance, inductance and the capacitance is determined by the following equations.

$$di_{dL}/dt = u_d/L + \omega i_{qL} \quad 2.23$$

$$di_{qL}/dt = u_q/L - \omega i_{dL} \quad 2.24$$

$$du_{dc}/dt = \omega u_q + i_{dc}/C \quad 2.25$$

$$du_{qc}/dt = -\omega u_d + i_{qc}/C \quad 2.26$$

$$i_{dR} = u_d/R \quad 2.27$$

$$i_{qR} = u_q/R \quad 2.28$$

where:

i_{dR} ,i_{qR}, i_{dL}, i_{qL}, and i_{dC}, i_{qC} are the d-axis and q-axis currents through the load resistance, inductance and capacitance, respectively;

u_d and u_q are d-axis and q-axis terminal voltage;

R, L, and C are the values of load resistance, capacitance and inductance, respectively.

The RLC load equivalent circuit in DQ is shown in Figure 2.4[11].

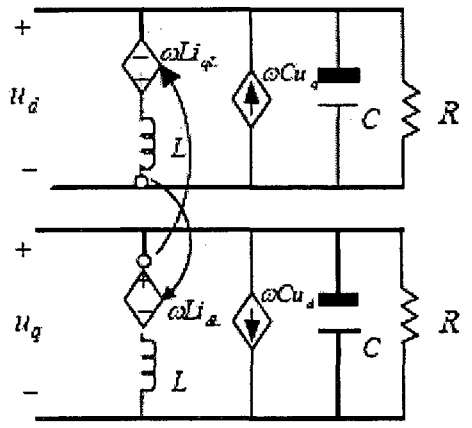

Figure 2.4 DQ equivalent circuit model of RLC load

Typically, motors consume up to 70% of the total energy supplied by a feeder. Therefore, the dynamics attributable to motors are usually the most significant aspects of dynamic characteristics of the overall system load. Motor loads, however, vary largely in characteristics due to different applications. The motor load used in the simulation studies described in this report is a compromise; it is intended to represent a general population of motors ranging in types from those in small residential/industrial applications to large motors. The default motor load uses only a single-cage representation. This is adequate for dynamic stability studies where damping of oscillations, rather than stalling of motors and motor starting, is the main focus.

The induction motor to be studied is represented by a standard single-cage model with the transient variations of its rotor flux linkage handled explicitly. The motor can be described by performance-based parameters or equivalent circuit parameters. The driven load is characterized by the inertia constant, H_m, of the combined motor-load rotor and

the exponent D, relating driven load to its speed. The detailed modeling of the motor load can be found in reference [9]. The dynamics of the induction motor is described by

$$e_{dm} = -1/T(e_{dm} + (X_{sm} - X'_{sm})i_{qm}) + p\theta_r e_{qm} \quad 2.29$$

$$e_{qm} = -1/T_o(e_{qm} - (X_{sm} - X'_{sm})i_{dm} - p\theta_r e_{dm} \quad 2.30$$

$$2H_m\omega_m = (e_{qm}i_{qm} + e_{dm}i_{dm}) - T_{norm}(\omega_m/\omega_o)^D \quad 2.31$$

where:

e_{dm} and e_{qm} are D-axis and q-axis components of the motor transient stator voltage;

i_{dm} and i_{qm} are d-axis and q-axis components of the motor transient stator current;

X_{sm} is the motor synchronous inductance;

X'_{sm} is the motor transient inductance;

H_m is inertia constant of the motor;

D is load model exponent of the motor;

T_{norm} is normal value of mechanical torque of the motor;

ω_m is rotating speed of the motor.

Figure 2.5 shows the DQ equivalent circuit of the induction motor.

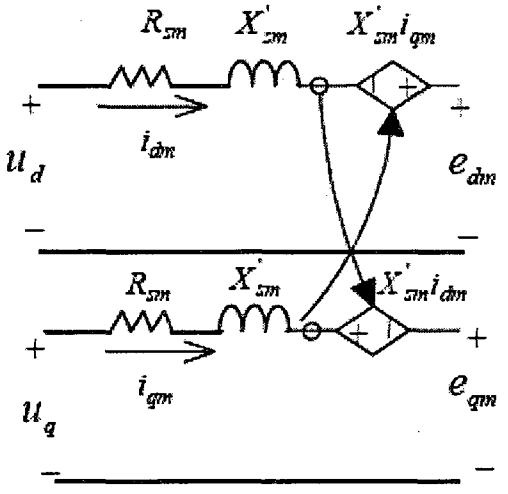

Figure 2.5 DQ equivalent circuit model of induction motor

2.6 Grid Model

Since the synchronous machine is connected to an infinite bus, the d-q terminal voltage of the machine is constrained by the grid voltage, described in DQ frame below [12]:

$$V_d = R_e i_{dgrid} + L_e i_{dgrid} - \omega L_e i_{qgrid} + V^{\infty} sin(\delta + \alpha) \quad 2.32$$

$$V_q = R_e i_{qgrid} + L_e I_{qgrid} + \omega L_e i_{dgrid} + V^{\infty} cos(\delta + \alpha) \quad 2.33$$

where:

R_e and L_e are the grid resistance and inductance respectively;

V^{∞} is the rms value of the bus voltage and α is its phase angle;

I_{dgrid} and i_{qgrid} are the d-axis and q-axis currents flowing into the grid.

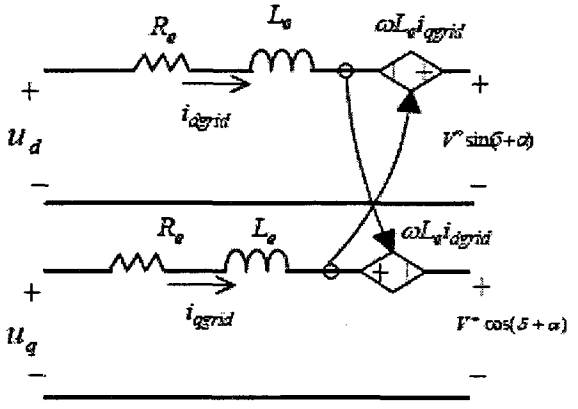

Figure 2.6 DQ equivalent circuit model of grid

Therefore, the highly nonlinear model can be greatly simplified and the dynamical characteristics of the power system can be approximately analyzed from the following small-signal model.

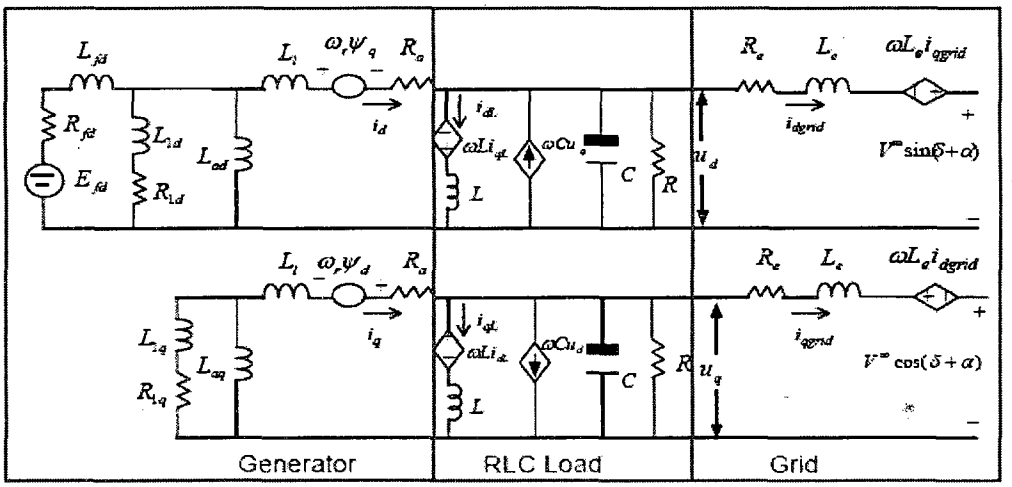

Figure 2.7 DQ equivalent circuit model of the overall system [11]

2.7 Model Implementation in Simulation Software

Synchronous generator equivalent circuit in the rotor reference frame, shown in Fig. 2.1, is very convenient to simulate with any software that allows schematic descriptions of electric circuits, since only resistors, inductors and current dependent voltage sources need to be implemented. MATLAB/SIMULINK was used for all simulation results in this thesis. Implementation of the circuit is straightforward, and only a few details will be given some attention in Chapter 4.

CHAPTER 3

NON-DETECTION ZONE

All anti-islanding schemes have some limitations that may include:

1. High implementation cost;
2. Need for coordination between the DG operator and the utility;
3. Susceptibility to false detection of islanding (nuisance tripping);
4. Possible non-detection of islanding under some conditions; and
5. Possible reduction of utility power quality and voltage and frequency stability.

Since anti-islanding schemes are not perfect and may impose financial or performance costs, it is necessary to understand the actual probability that an island will occur and what risks this unintentional island will present to human safety and the electrical network. This allows the benefits of further risk reduction from better anti-islanding schemes to be balanced against the costs imposed by these schemes. If a simple and low cost anti-islanding scheme reduces risk to a level below other electrical safety risks that are currently considered acceptable, it is debatable whether a scheme with better detection performance, but higher costs (in financial or performance terms), is necessary.

3.1 Importance of Determining Non-Detection Zone

One of the main limitations with local detection schemes is that each scheme has an operating region where islanding conditions cannot be detected in a timely manner. This region is called the non-detection zone (NDZ). The impact of the non-detection zone can be negligible in some cases and can be significant in other cases. The frequency-based anti-islanding methods, which are the most commonly employed schemes for synchronous generators, are used here as an example to illustrate the risks associated with the non-detection zone.

The frequency-based anti-islanding scheme uses locally measured frequency as a criterion to decide if an island is formed. It is known that when a feeder is connected to the utility supply, the feeder frequency is almost constant. On the other hand, the frequency of an islanded feeder can have various values depending on the power mismatch between the load and generation in the island. Excess generation will drive up the frequency and deficit generation will result in the decline of frequency. Accordingly, if there is a large power mismatch in an island, the frequency based anti-islanding scheme will be able to detect islanding condition quickly. If the power mismatch is small, however, it will take longer time to detect the islanding condition. In the extreme case where the load and generation in the islanded system are very close, the devices could fail to detect an islanding situation within the allowed time period. Thus, the non-detection zone can be specified using the power mismatch level in an island.

Two factors can significantly affect the power mismatch levels in an island. The first factor is the daily variation of feeder loads. Depending on their operating characteristics, feeder loads could have $\pm 20\%$ variation around its daily average. The

second factor is that different islands could be formed with a DG. Each island will have different load levels. Both factors will work together to create more situations where small power mismatch levels could be encountered, leading to increased risk of non-detection. This situation is illustrated in Figure 3.1 below.

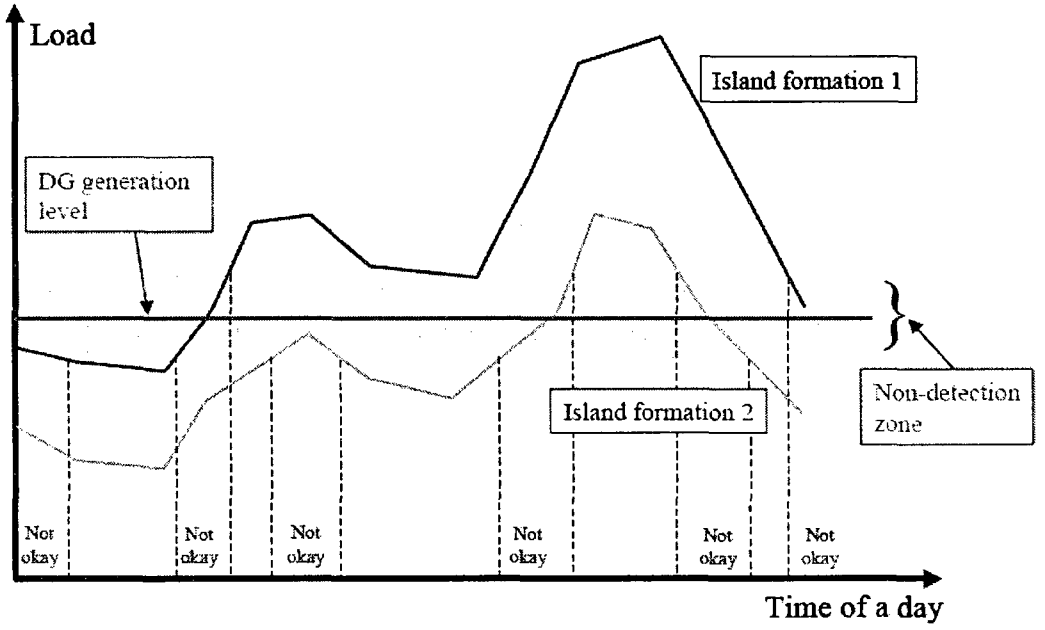

Figure 3.1 Non-detection zone relative to load variation

The figure shows the variation of load level during a 24-hour period. Two load variation curves are shown. Each curve corresponds to a different island formation scenario. The power output of the DG is assumed as constant during the 24-hour period. So it is a horizontal line. The intersections of the DG curve and the load variation curves represent the cases where there is a zero mismatch between load and generation. The non-detection zone is shown as a shaded band. Any load values that fall into the band will result in poor detection of islanding conditions (marked as 'not okay' in the figure). It

can be seen that there are a number of operating periods during which poor or no detection of islanding conditions can occur. If more islanding scenarios are added (i.e. if there are more load variation curves), such periods will increase further. A frequency-based relay can be used reliably only if the distributed generator is less than about half of the smallest load in any possible island formations.

3.2 Risks Associated with Non-Detection Zones

The probability of islanding and the risks associated with the formation of an island are typically less for inverter based DGs than for synchronous generator based DGs.

An island is sustained only while there is a relatively close match between the power output of the DG and the power consumption of the load within the island. Long duration islands are much less likely than short duration islands since both DG power output and load power consumption change with time. Most studies on the risks associated with islanding of inverter based DGs have found that islands lasting more than a few minutes are very unlikely. Therefore this risk is more of an issue with automatic service restoration techniques, such as automatic reclosing, than with manual reconnection.

The hazard to utility line-workers or other personnel by causing a line to remain energized that may be assumed to be disconnected from all energy sources is commonly viewed as the most serious risk of islanding since it involves human safety rather than potential equipment damage or malfunction. As a result, this risk has had the most extensive analysis. The risk to utility line workers can be mitigated by following

established rules for line maintenance and repairs. With line workers operating under established hot-line rules or deadline rules, an islanding situation will not increase the probability for line-worker hazards if those rules are followed. However, other personnel, especially emergency responders, such as firefighters, may not have the time or the capability to follow such procedures. Therefore there is a potential personnel hazard if an island persists beyond a few seconds. North American standards on DG islanding detection reflect this concern in their short trip time requirements.

As with the synchronous generator DG equipped with a frequency-based relay, an inverter based DG will only island if there is a relatively close match between the active and reactive power output of the DG and the active and reactive power consumption of the local loads within the isolation boundary. If there is a significant mismatch, the island voltage or frequency will shift outside the protective function's preset limits and the inverter will cease to energize or the protective relay will cause the DG to disconnect.

3.3 Determination of Non-Detection Zone for the System

The idea of using graphical tools to evaluate the effectiveness of frequency and voltage relays for distributed generation anti-islanding protection has its origin in earlier papers, such as in [6] and [7]. The method employed in [7] consisted of a voltage-frequency window defined by the voltage and frequency relays settings. By using such a method, one can analyze the relays operation through the voltage-frequency paths described during an islanding event, including phenomena as generator self-excitation and ferro-resonance. While the trajectory described by the voltage-frequency signal remained inside the voltage-frequency window, the relays were not activated. In spite of

the usefulness of the voltage-frequency window method presented in [7], such method does not bring information about the active and reactive power imbalances that cause frequency and voltage deviations. This information in addition to the relays settings can improve the understanding about the anti-islanding system operating performance, since the power imbalance conditions that do not cause relay operation can be previously known. This is the basic idea behind the non-detection zones in the power mismatch plane.

There are two aspects of power imbalance in an island. One is the active power imbalance and the other is the reactive power imbalance. Any particular power imbalance situation in an island can therefore be presented as a point in the ΔP and ΔQ in plane.

The following is the system used for simulation and it is tried to determine the Non-detection zone of the power system.

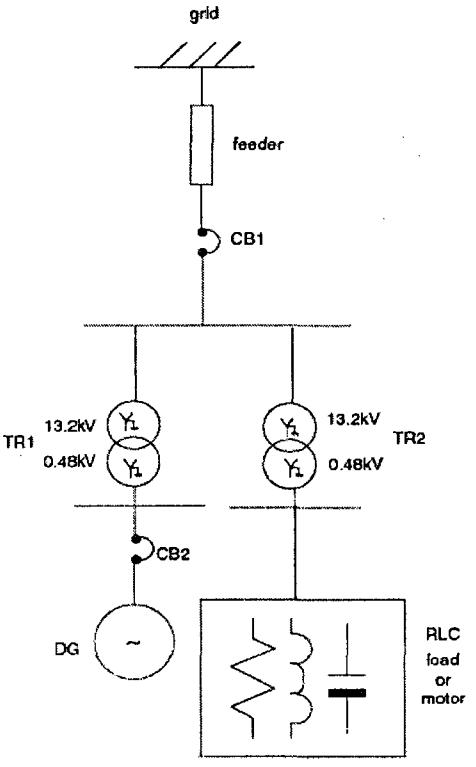

Figure 3.2 Single line diagram of system [11]

To determine the non-detection zone, the active and reactive power imbalances are varied from -1 to 1 p.u. by changing the load-generation scenario of the electrical system. The power basis used is the synchronous machine rated power. The following parameters are sample parameters utilized to define the shape and size of the NDZ of a sample frequency based relay:

- Required islanding detection time: 500 ms;
- Load type: constant power;
- Generator excitation system: voltage control;
- Permissible steady-state voltage (0.95/1.05 p.u.);

- Relay setting: 57.5 Hz for under frequency cases and 62.5 Hz for over frequency ones.

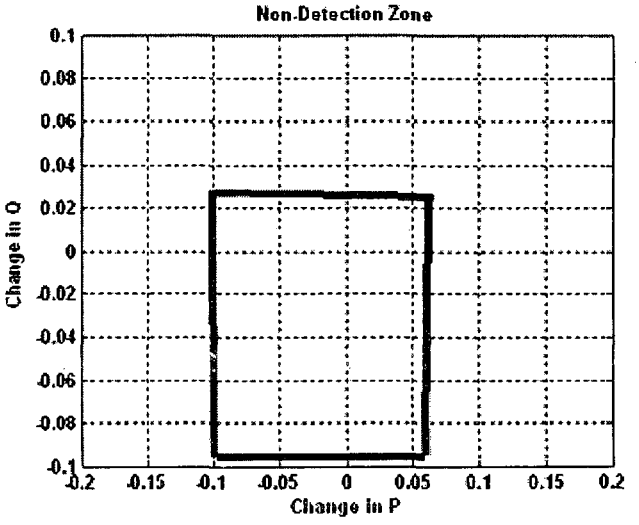

Figure 3.3 Non-detection zone for a frequency relay

The non-detection zones of frequency-based and voltage relays employed for anti-islanding protection of synchronous DG are important to characterize the capabilities and limitations of such devices, so that they can be more effectively adjusted and evaluated.

Voltage relays are not suitable to detect the islanding of a synchronous DG if the excitation system is configured to the control terminal voltage. In this case, the associated NDZ may be as big as the feasible operating region for some operating conditions, even for sensitive settings. Therefore, with the non-detection zone of a frequency relay known for the system and the voltage relays incapability of detecting islanding conditions, it is tried to show that a positive feedback anti-islanding scheme is capable of avoiding the NDZs.

CHAPTER 4

POSITIVE FEEDBACK ANTI-ISLANDING SCHEME

4.1 Introduction of Positive Feedback

The proposed Anti-islanding schemes for the synchronous machine DG are implemented on the basis of a positive feedback. The principle behind the method is to destabilize frequency or voltage by introducing positive feedback. This result in under/over frequency or voltage trip varies quickly once the DG is islanded. In the presence of the grid, the positive feedback will have little effect on the grid frequency or voltage regulation. In contrast to the passive methods, these active schemes can detect islanding effectively and reliably without causing false trip.

Although the positive feedback concept has been successfully used for the inverter-based DG for AI protection, the application of the concept to synchronous machine has not yet been explored extensively [3]. Typically, a rotating-machine-based DG is characterized by higher inertia—longer time constants than an inverter-based DG. Due to these factors, the machine and the inverter-based DG respond in fundamentally different ways.

In support of the design and implementation, both frequency-domain and the time-domain analysis are conducted to provide the insights into the characteristics of the proposed schemes.

4.2 Implementation of the Active/Reactive Power Schemes

The positive feedback for the synchronous machine comes in two different ways, denoted as active power AI scheme and reactive power AI scheme; because the feedback modifies the active power and reactive power references, respectively. The structures of the active and reactive power AI scheme are shown in Fig. 4-1. The active power AI compensator takes the variations in the frequency as input to modify the active power reference to the DG. The reactive power AI compensator uses the variation in the voltage magnitude to change the reactive power reference.

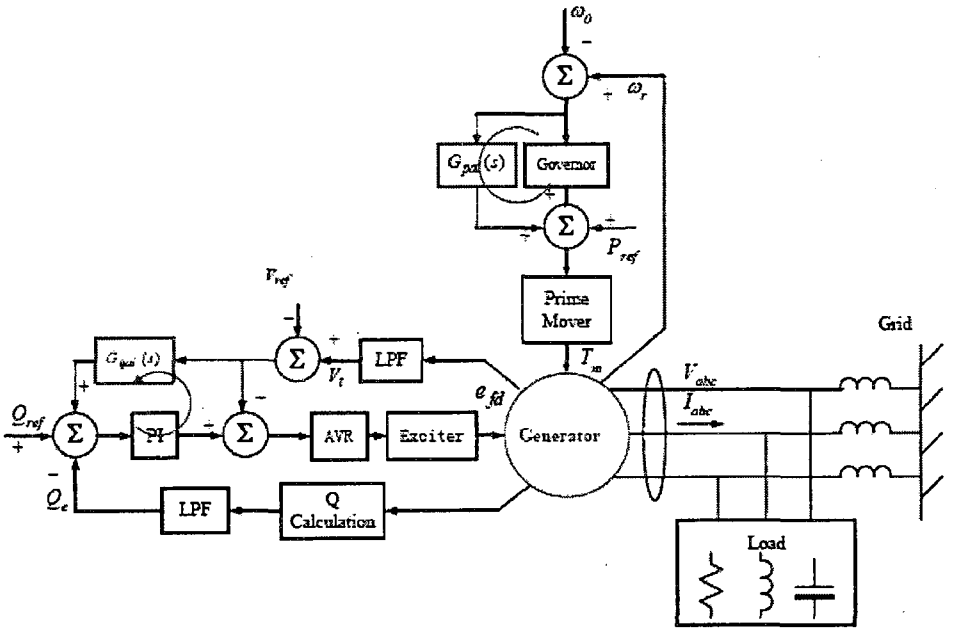

Figure 4.1 Schematic of the machine with the AI compensators [11]

The AI compensators both consist of a washout filter and a proportional gain. The washout filter is designed to ensure that the AI compensators only react to the transient of the frequency/voltage, but not causing any DC steady-state error. When there is a very

small or substantial voltage or frequency variation, the responses of the AI loop will amplify the voltage or frequency variation in the same direction. Therefore, the loops are called positive feedback. The mechanism can be further illustrated below.

When there is a generator terminal voltage variation, for instance, voltage increases slightly, and the reactive power reference will be increased due to the reactive power AI loop, which will lead to a boosted voltage reference, thus causing the terminal voltage to further increase. When properly designed, the effect of the reactive power AI loop is insignificant when the grid is connected because the grid will regulate the terminal voltage magnitude. Once the grid is lost, the reactive power AI loop becomes dominant and drives the voltage away from nominal.

A similar mechanism applies to the frequency. When there is a generator speed (frequency) variation, e.g., when frequency increases slightly (due to under loading), the active power reference will be increased due to the active power AI loop, which will further generate a greater mechanical torque (resulting in more under loading), causing higher speed (frequency). When properly designed, the mechanism will create this instability only in an islanded system and cause a frequency relay to trip.

In summary, the main idea is that the active/reactive power AI compensators have a dominant effect in the frequency/voltage oscillations when the grid connection is lost. But, with a proper design, these destabilization effects are negligible, when the machine is connected to the grid.

4.3 Design Guideline based on Frequency-Domain Analysis

The basic principles of the positive feedback for islanding detection have been introduced. This section will emphasize on the design and implementation of the AI compensator. In order to illustrate the design guideline, a loop gain concept is used. MATLAB is used for the following frequency-domain analysis.

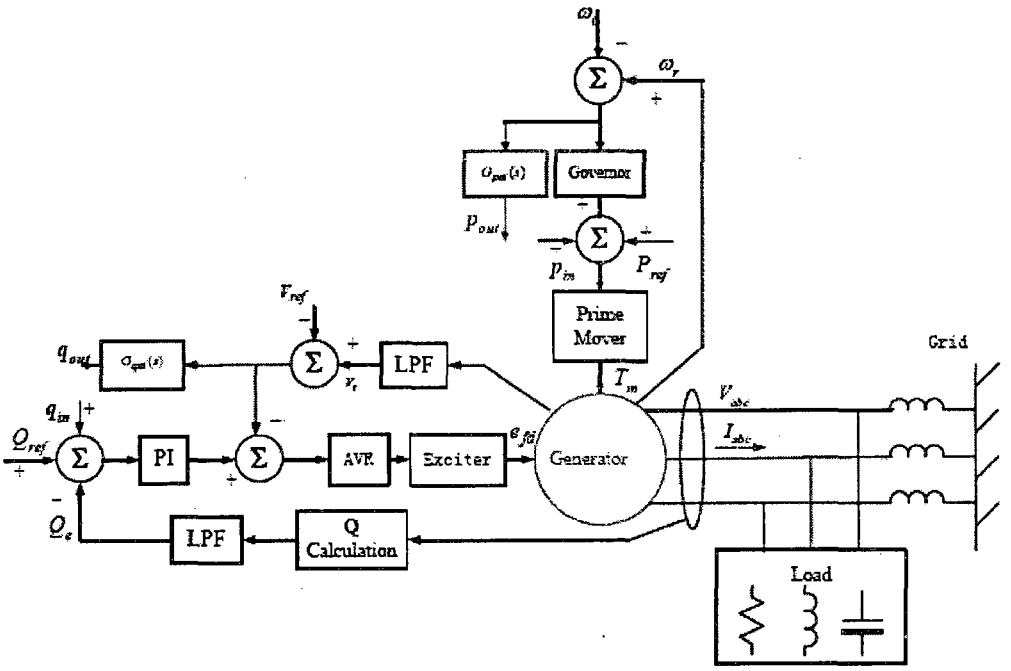

Figure 4.2 Schematic of the machine with the AI loops opened [11]

The loop gains of the active and reactive AI loops can be measured by breaking the loops, shown in Figure 10, where p_{in} and p_{out} are at the breaking point for the active power loop, while q_{in} and q_{out} are for the reactive power loop. The loop gain is defined as the small-signal transfer function from the perturbation signal p_{in} (or q_{in}) to the output p_{out} (or q_{out}). Therefore, the active power loop gain is given by:

$$Tp(s) = \frac{Pout}{Pin} \tag{4.1}$$

Similarly, the reactive power AI loop gain is defined as the small signal transfer function from the perturbation signal from q_{in} to the output $q_{out.}$

$$Tq(s) = \frac{qout}{qin} \tag{4.2}$$

From the loop gain, the system dynamics can be characterized by, for example, the stability margins. For AI control, the design principles are as follows:

(1) When the grid is connected, the loop gain should indicate a stable system, i.e., the peak of the AI loop gain must be less than 0dB. The lower the loop gain is below 0dB, the less impact of the AI loop on the DG's normal grid-connected operation.

(2) When the grid is disconnected, the loop gain should indicate an unstable system, i.e., the peak of the AI loop gain must be greater than 0dB, while the phase is lagging more than 180 degrees. The unstable system will ensure that the islanded system can be detected even when there is 100% active and reactive power matching. The higher the loop gain, the more quickly the island voltage or frequency will move outside the normal operational windows to trigger voltage or frequency protection. However, the gain should not be too high to insure that criterion (1) is met. Basically, criterion (1) sets the upper bound of the loop gain, while criterion (2) sets the lower bound of the loop gain.

If both criteria are satisfied, the AI compensator will amplify the frequency/voltage transients when the machine is islanded but with minimal effect on the frequency/voltage dynamics when the grid is connected.

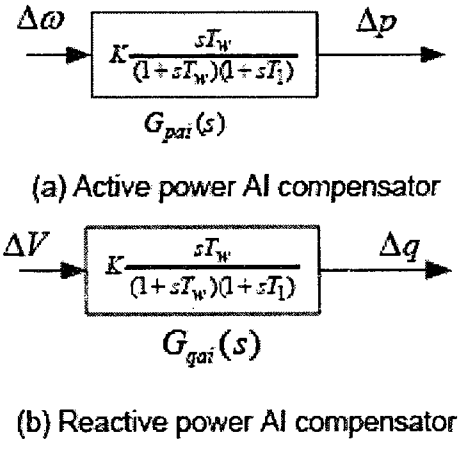

Figure 4.3 Active and reactive AI compensators [11]

Figure 4.3 shows the transfer function of the active/reactive power AI compensator. The AI compensator basically consists of a washout filter, a gain and a first-order filter. The crucial step in the design is to determine the setting for the active/reactive power AI compensator. The critical settings include:

(1) The corner frequency of the washout filter, T_w

(2) The gain, K

(3) The low pass filter corner frequency T_1

The washout function serves as a high-pass filter, with a time constant T_w to allow signals with frequency higher than $1/T_w$ to pass. For the signal with frequency lower than $1/T_w$, especially for DC signal, will be attenuated by the washout filter. This is to minimize the AI loop impact on the steady-state regulation. The low pass filter corner

frequency T_l is set to attenuate high-frequency noise. The combined washout filter and the low-pass filter constitute a band-pass filter. The selection of gain, K is a compromise between the high enough gain to ensure islanding detection quickly and the low enough gain to have minimal impact on the DG under the grid-connected conditions. The gain selection should leave certain margins for both grid-connected and islanded conditions.

4.3.1 Practical Design Considerations

The basic criteria for the AI design have been discussed. However, the parametric design of the AI compensator is still an issue since the active/reactive power loop gains may vary with the different load conditions. In order to ensure that the AI control is effective under all circumstances, the AI compensator must be designed under the worst-case situation. The critical gain can only be approximately determined after the study of a range of different load conditions. Consequently, the impact of the various passive and motor load conditions on the loop gains must also be examined. The preliminary study concludes that the situations important to this AI scheme design are those where the grid impedance is high or there is a high penetration of induction motor load.

After the worst cases have been identified, the active and reactive power AI compensators are chosen for the particular system simulated as:

$$\frac{\Delta P}{\Delta \omega} = \frac{2s}{[(0.032s+1)(0.029s+1)]} \tag{4.3}$$

$$\frac{\Delta Q}{\Delta V} = \frac{2.41s}{[(0.048s+1)(0.016s+1)]} \tag{4.4}$$

When the analysis of the loop gains is carried out in the following, it is assumed that:

1. The power output of the machine and the local load are closely matched.

2. The machine operates at a power factor of 1.0 (due to the choice of the RLC load with unity power factor).
3. The tripping the utility breaker at a moment when the system is operating at steady state causes the loss of the grid.

4.4 Performance Evaluation with Frequency-Domain Simulations

With the above assumptions, the impact of three different factors (power level, load quality factor, and motor load) on the proposed AI schemes is investigated.

4.4.1 Power Level

In order to examine the impact of the different power level on the loop gain, the generator active power, which matches the active power of the RLC load (with Qf=1.0), is varied from 50% to 100%. The Bode plots of the loop gains under different power levels are shown in Figure 4.4.

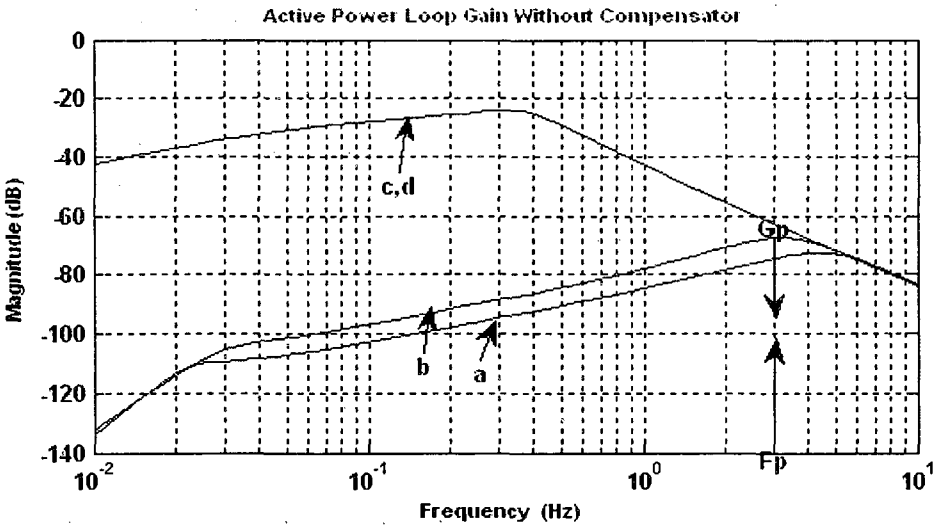

(1): (a) (b) Grid-connected: with 50% DG power output, 100% DG power output;

(c) (d) Grid-disconnected: with 50% DG power output, 100% DG power output

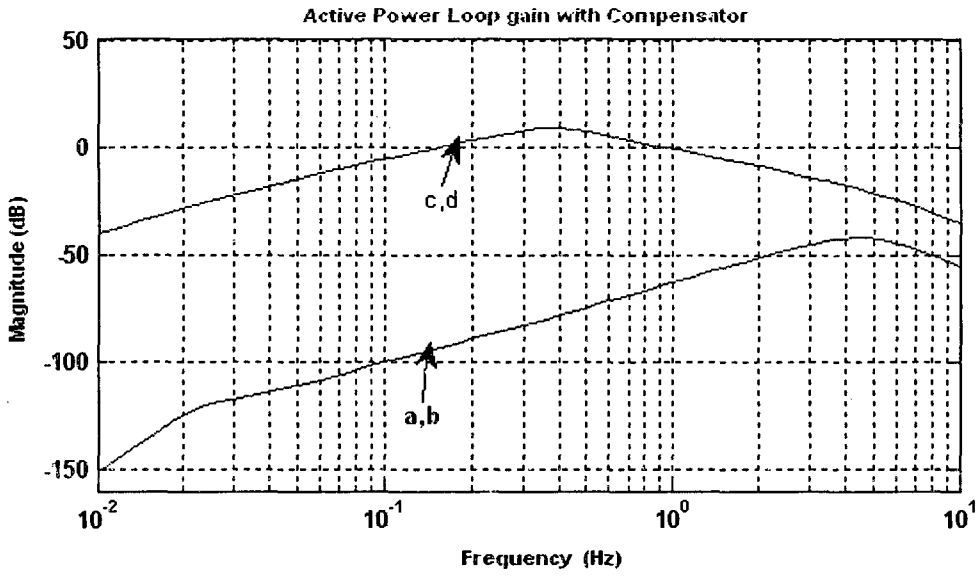

(2): (a), (b) Grid-connected: with 50% DG power output, 100% DG power output;

(c), (d) Grid-disconnected: with 50% DG power output, 100% DG power output

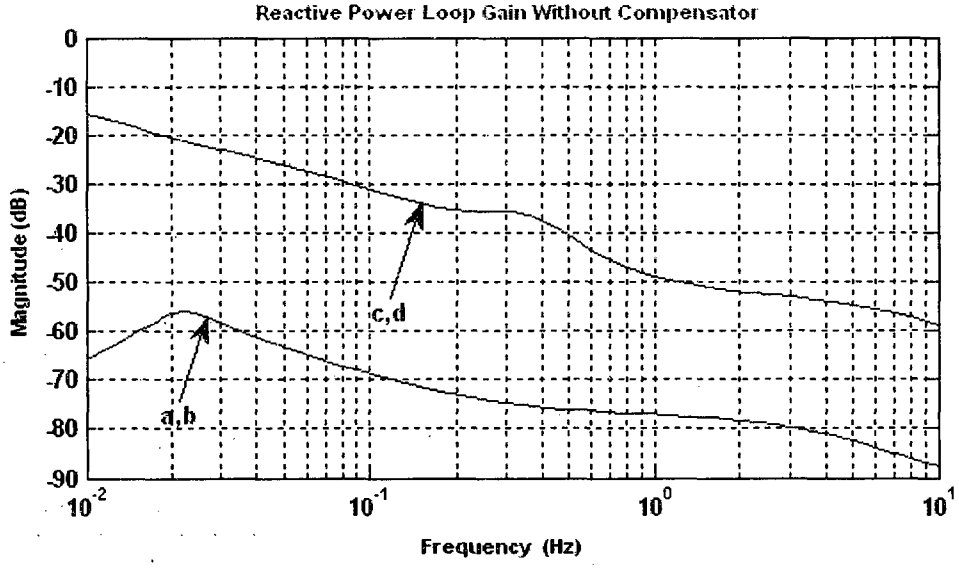

(3): (a), (b) Grid-connected: with 50% DG power output, 100% DG power output;

(c), (d) Grid-disconnected: with 50% DG power output, 100% DG power output

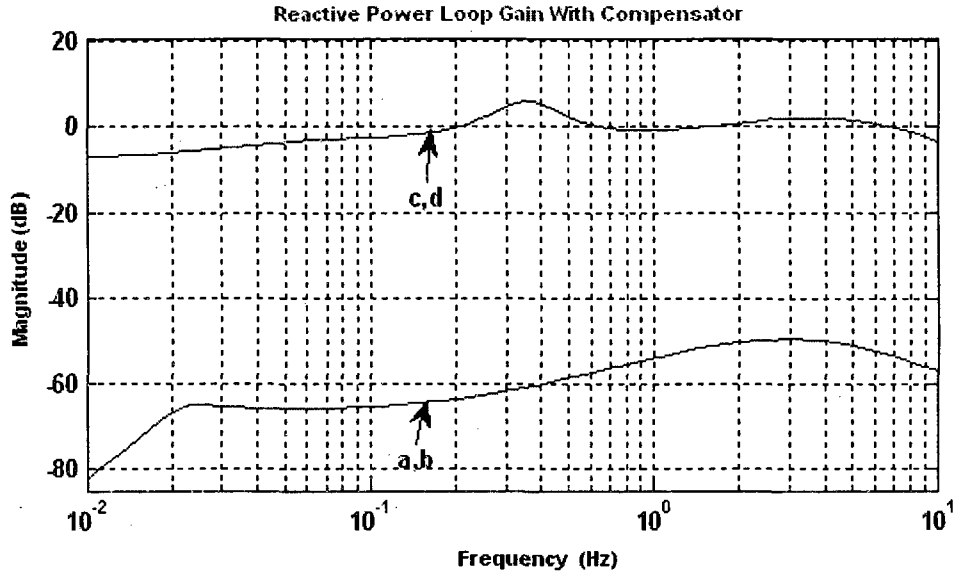

(4): (a), (b) Grid-connected: with 50% DG power output, 100% DG power output; (c), (d) Grid-disconnected: with 50% DG power output, 100% DG power output

Figure 4.4 Loop Gains with different DG output power

Without any compensator, both the active power and reactive power loop gains are much less than 0dB, under both grid connected cases and islanded conditions cases. The gain below 0 dB even when the grid is disconnected implies that the isolated DG and load system is stable, thus can be islanded. It is consistent with the time-domain simulation results in a later section that show, without any compensator, the islanding can be easily sustained.

After being compensated, both the active power and reactive power loop gains are reshaped. The compensator design should be such that, the grid-connected loop gains are below 0dB in order to keep the system stable, while the islanded loop gains are above 0dB in order for effective AI detection. For the purpose of illustration, the peak value of

the open loop gain is denoted as Gp, and the corresponding frequency is called Fp. Basically Gp and Fp together determine the dynamic characteristics of the AI control. From the design point of view, the larger Fp and Gp, the stronger the dynamics of the islanded system. However, there are some fundamental limits on the maxima of Fp and Gp. For the active power AI scheme, the limit on is due to the inertia of the DG. In this design, Fp under the grid-disconnected condition is very small. This small Fp indicates the slow response of the active power AI scheme to the loss of the grid. In order to overcome the slow response due to small Fp, a high gain is necessary so that the frequency can be effectively driven out of the normal range for a given time. However, a high gain may potentially cause the DG instability, which sets the upper bound of the loop gain.

From the Bode plot shown in Figure 4.4 (4) bottom figure, it can be seen that the Fp of the reactive power AI loop gain is smaller than that of the active power AI loop gain. In this case, the gain can be higher than the gain for the active power loop gain. This indicates that the reactive power AI scheme can respond slower than the active power AI scheme.

Another observation is that, once the rotating-machine-based DG is islanded, the difference in the loop gain due to the different power levels is insignificant.

4.4.2 Quality Factor

The loop gains with the different quality factors of the load, Qf=0.0 and Qf=1.8, are compared with each other in Figure 4.5. The quality factor of a RLC load is defined as the ratio of the reactive power stored in the load inductor or capacitor to real power consumed by the resistor. For a load with fixed active power, the different quality factors

imply varying the reactive power of the load, i.e. inductance and capacitance. Usually, a load with the quality factor of 1.8 is considered an extreme case for the islanding study. From Figure 4.5, it can be seen that the loop gains vary little with different quality factors for both grid-connected and islanded conditions. Generally, Qf represents the load inertia. The machine-based DG has large inertia and dominates the overall DG/load system inertia. As a result, different Qf makes little difference in the system dynamics.

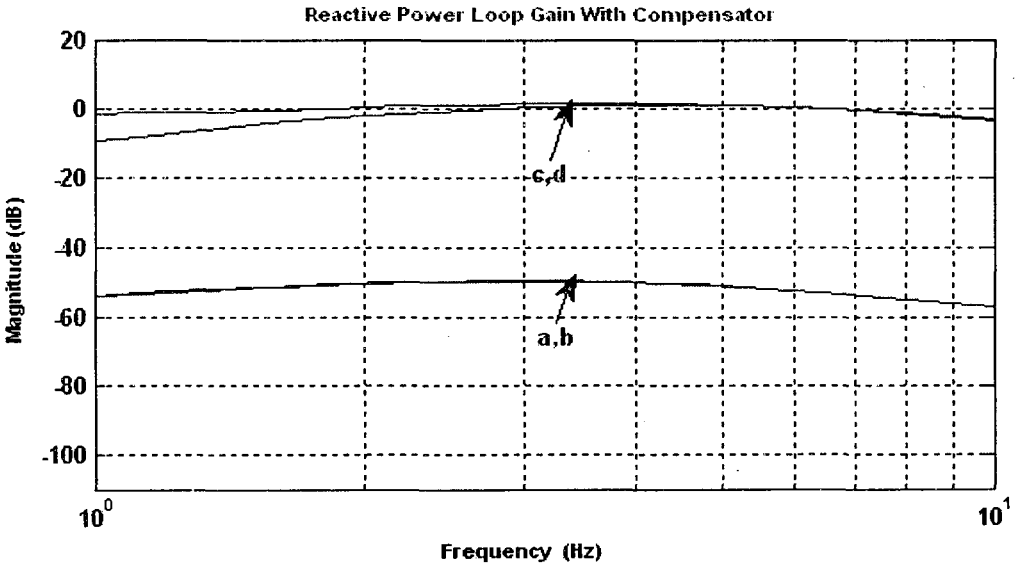

(1): (a), (b) Grid-connected: load Qf=0.0 and Qf=1.8; (c), (d) Grid disconnected: load Qf=0.0 and Qf=1.8

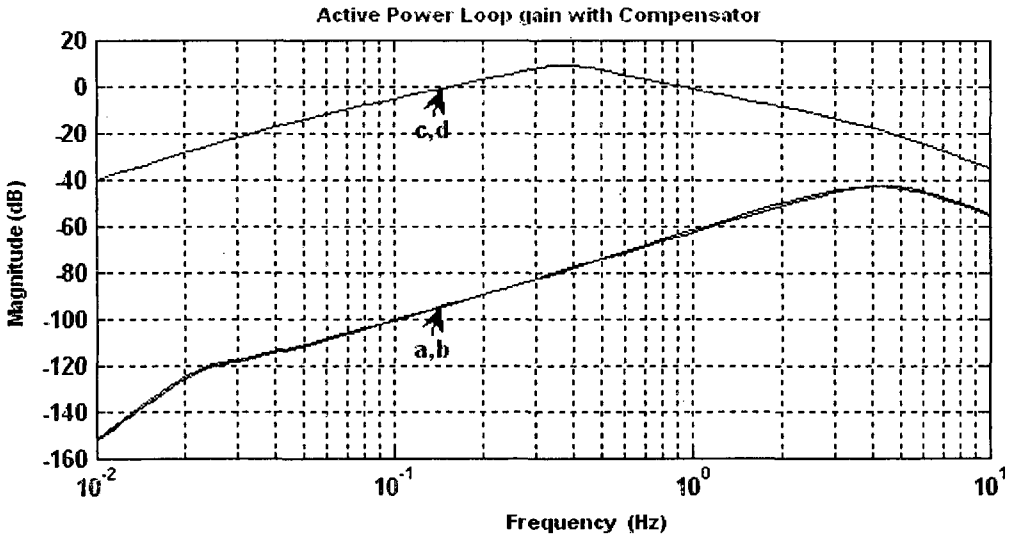

(2): (a), (b) Grid-connected: load Qf=0.0 and Qf=1.8; (c), (d) Grid disconnected: load Qf=0.0 and Qf=1.8

Figure 4.5 Loop gains with different Quality factors

4.4.3 Motor Load

Induction motors constitute a major part of the distribution load. Studies [9] show that the most important sensitivity influencing the system dynamics is the percentage of motors in a feeder. Variations in the motor inertia and impedances are not as great an influence on the system dynamics as the percentage of motors. The effects of the motor load on active/reactive power loop gains are evaluated when the load is composed of an induction motor (Power Rating=150kVA, comparable to the generator rating) and a capacitor for power factor correction.

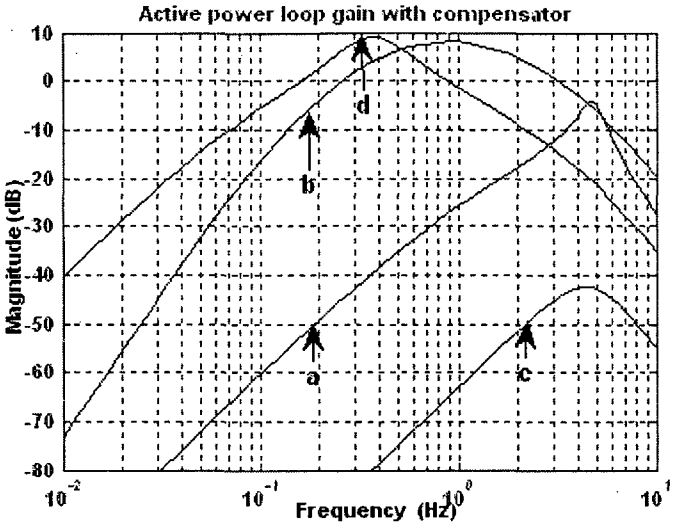

(1): (a), (b) Grid-connected/disconnected motor load (P=0.5 pu and Qf=1.8); (c), (d) Grid-connected/disconnected RLC load (P=0.5 pu and Qf=1.8)

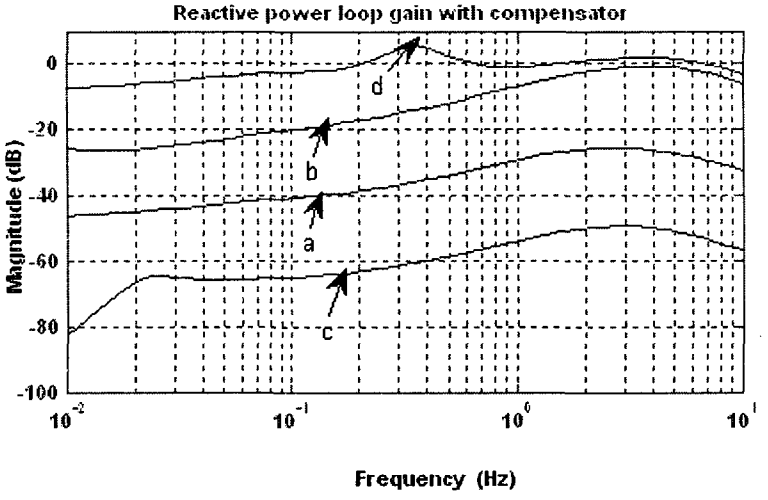

(2): (a), (b) Grid-connected/disconnected motor load (P=0.5 pu and Qf=1.8); (c), (d) Grid-connected/disconnected RLC load (P=0.5 pu and Qf=1.8)

Figure 4.6 Loop gains with RLC and Motor load

Figure 4.6 shows the loop gains comparison between RLC load and motor load (with capacitor), both at unity power factor with the same power level. It can be seen that the active power loop gain of the induction motor load is lower than the loop gain with the RLC load. It implies that the induction motor load slows the dynamics of the islanded system down. In contrast, the reactive power AI scheme is still very effective with the motor load. It indicates that the motor load is a worse case than RLC load for the active power scheme. For reactive power scheme, however, the motor load is easier to detect than the RLC load.

4.5 Performance Evaluation with Time-Domain Simulations

In the preceding sections, the basic principles and design guidelines of the proposed two AI schemes have been discussed. In this section, time-domain simulations are carried out using MATLAB/SIMULINK to validate the proposed schemes and to evaluate their effectiveness. The parameters of the DG and the load used in the simulations are given in the Appendix. The system used in the simulation consists of grid, synchronous generator, and RLC or motor loads. A constant voltage source behind impedance is used to represent the grid. The local load and the DG are closely balanced. The loss of the grid is due to the trip of a utility breaker at steady state, and this is considered as the worst case for islanding detection.

The performance of the AI schemes is evaluated for both a static load and the induction machine load. For all islanding simulations, the grid is disconnected at t=15s.

4.5.1 Performance Evaluation with Resistive Load

Before evaluating the performance of the proposed AI schemes, a baseline case with the grid-connected and AI schemes included is simulated, shown in Figure 4.7.

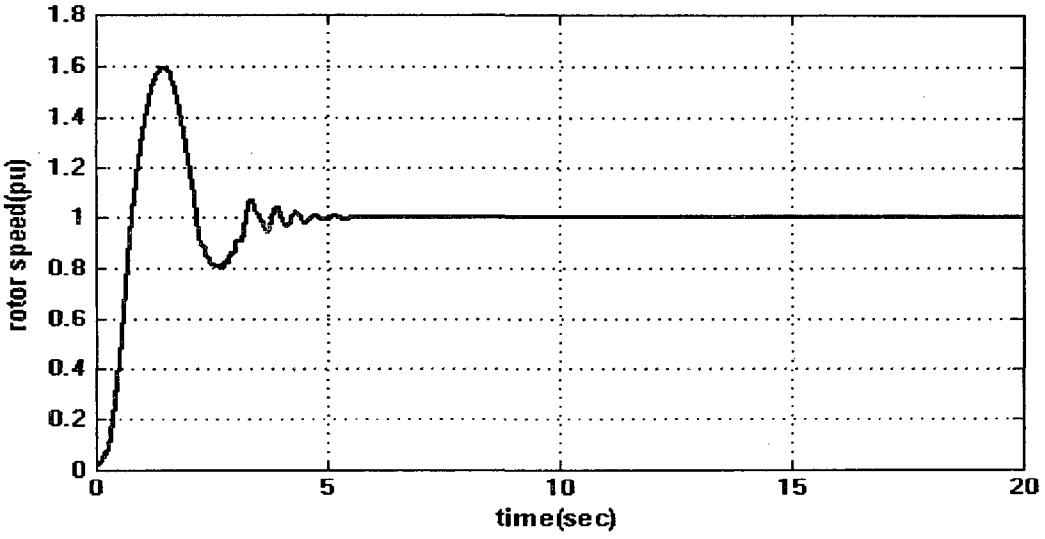

(a) Rotor speed (pu)

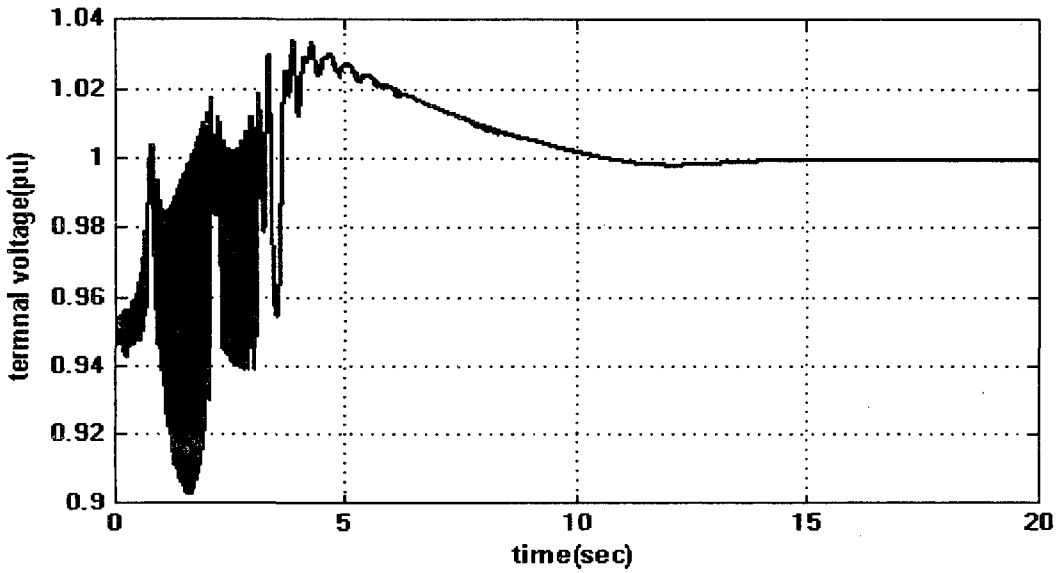

(b) Terminal voltage (pu)

Figure 4.7 Simulation result with grid-connected and AI schemes included

For the case with AI schemes enabled, the DG is operating at 150 kW, 100% of its rated power and a resistive load of 150 kW (100%) or 112.5 kW (75%) has been simulated. Since the load and the DG are closely matched, the island can be sustained after the loss of the grid, because the variation in the frequency and the terminal voltage is so small that any passive scheme may not detect the islanding.

The simulation results are shown in Figure 4.8. After the grid disconnection at t=15s, the rotor speed drifts quickly (within 2s) to go out of normal ranges.

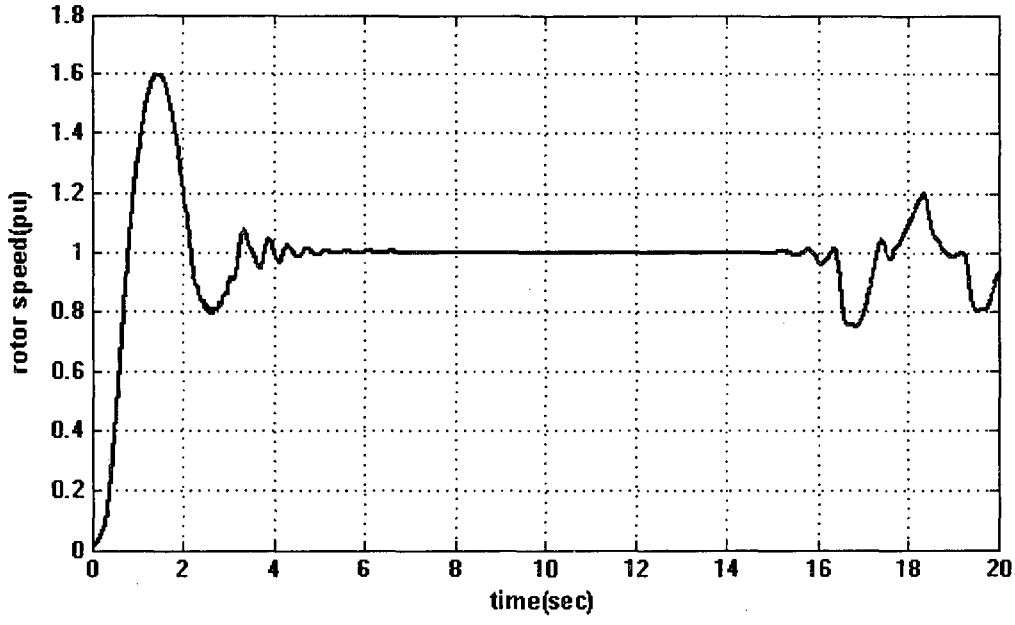

(a) Rotor speed (pu) at 100% of the rated load

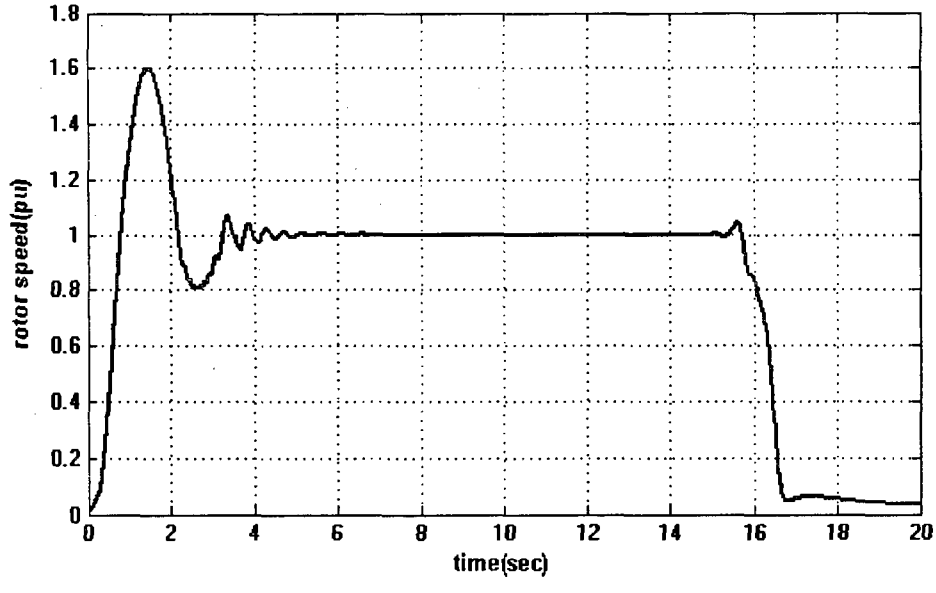

(b) Rotor speed (pu) at 75% of rated load

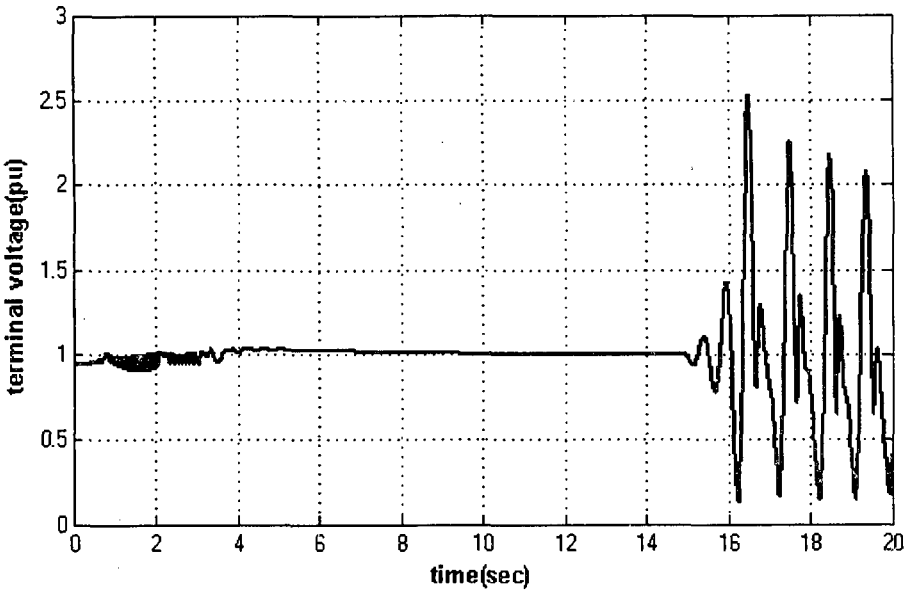

(c) Terminal voltage (pu) at 100% of rated load

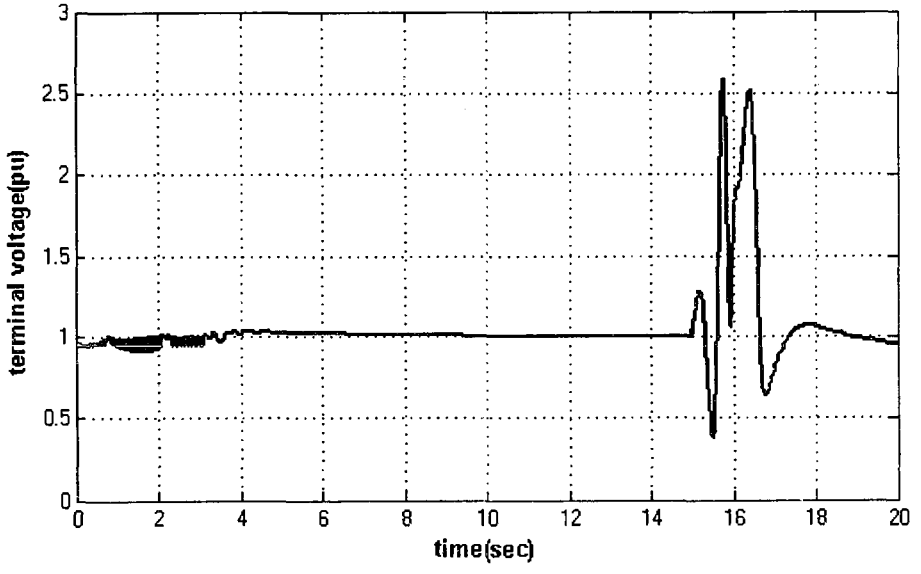

(d)Terminal voltage (pu) at 75% of the rated load

Figure 4.8 Simulation results for resistive loads (t=15sec)

As can be seen from the figure above, for a load that is not closely matched both the active and reactive power AI schemes respond sufficiently for OV/OF relays. But for a closely matched loading, the reactive power AI scheme responds strongly while the active power AI scheme responds slowly.

4.5.2 Performance Evaluation with RL Load

The DG is operating at 150 kW, 100% of its rated power. The Resistive-Inductive load is 72.5 kW-131.124KVar/54.6KW-98Kvar with the active power and reactive AI schemes enabled have been simulated.

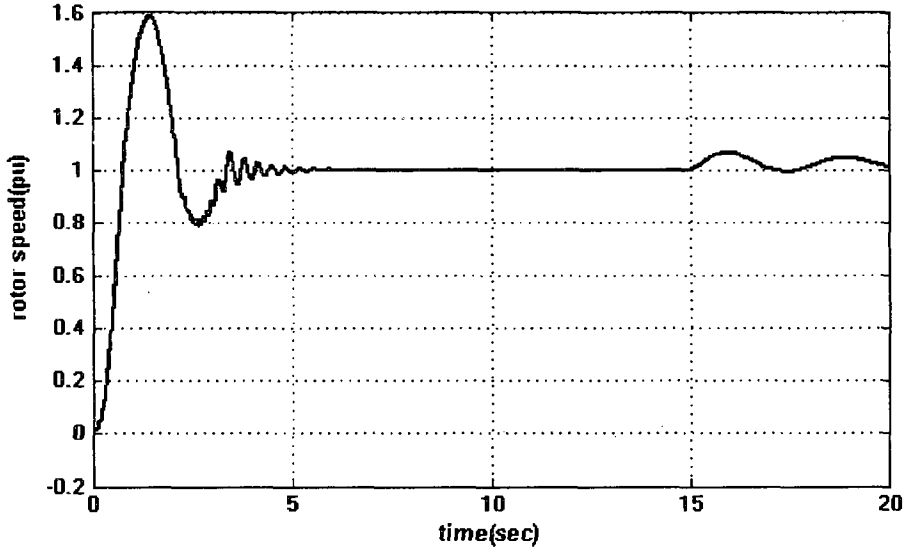

(a) Rotor speed (pu) with 100% of rated load

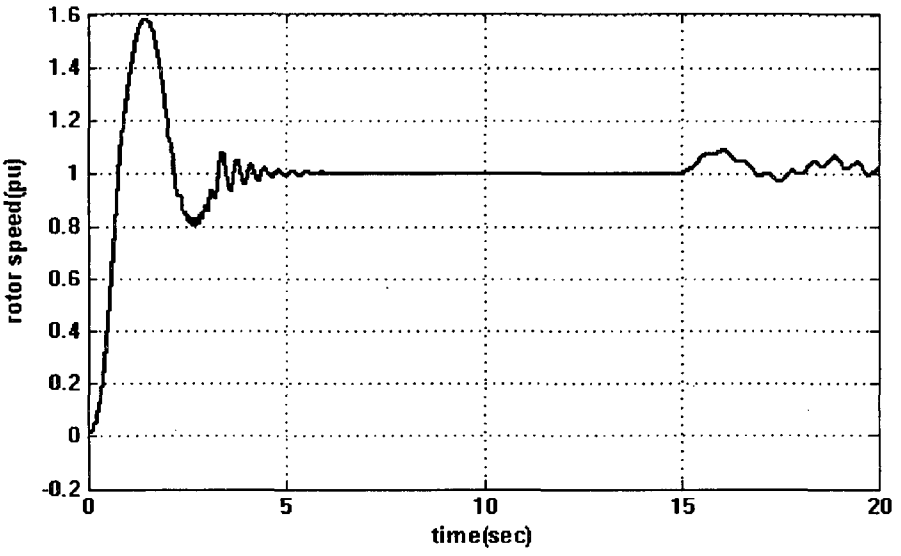

(b) Rotor speed (pu) with 75% of rated load

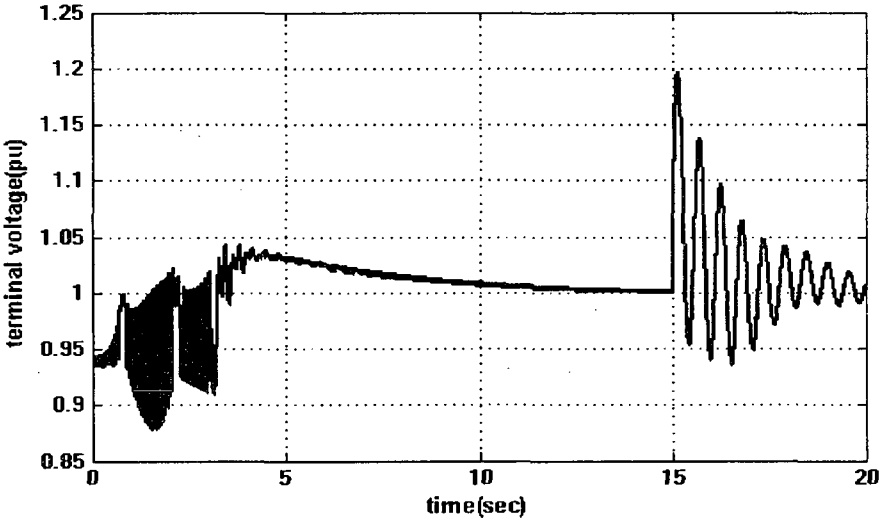

(c) Terminal voltage (pu) with 100% of rated load

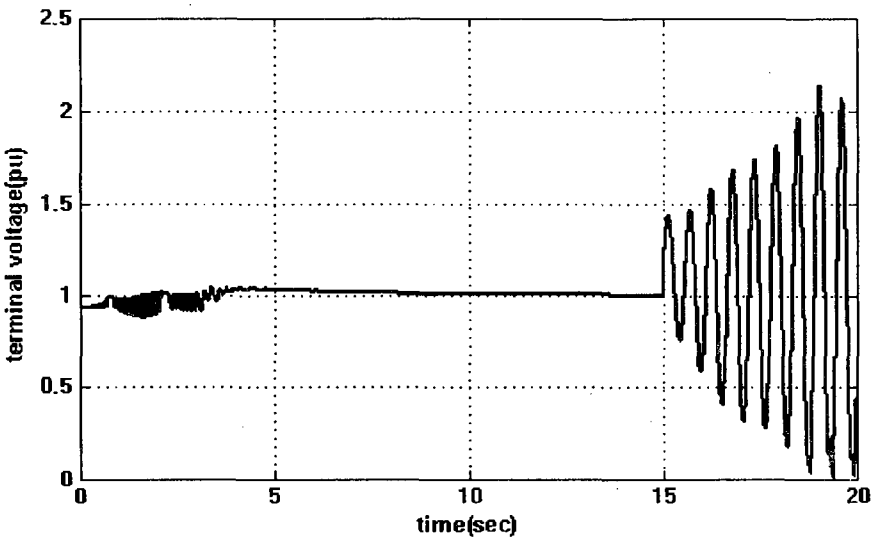

(d) Terminal voltage (pu) with 75% of rated load

Figure 4.9 Simulation results for R-L load (t=15sec)

The simulations of the RL load shows that both AI schemes react with the way as they reacted with a resistive load.

4.5.3 Performance Evaluation with RLC Load

The DG is operating at 150 kW, 100% of its rated power. The RLC load is 150 kW/112.5KW with quality factor Q_f=1.8. The same DG output and different loading conditions, but with the active power and reactive AI schemes enabled, has been simulated. The simulation results are shown in Figure 4.7. After the grid disconnection at t=15s, the terminal voltage drifts quickly (within 2s) to go out of normal ranges.

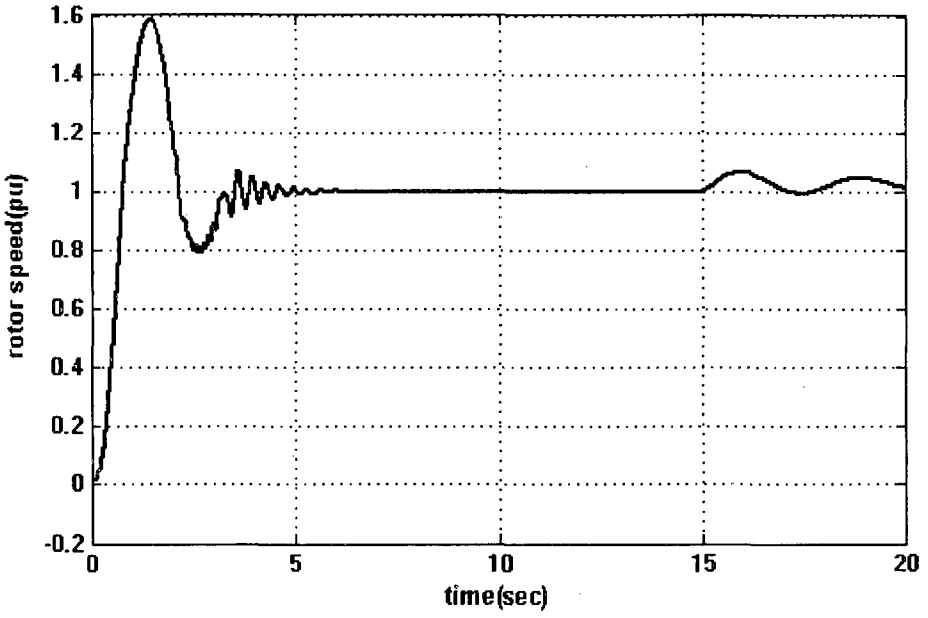

(a) Rotor speed (pu) with 100% of rated load and load Q_f=1.8

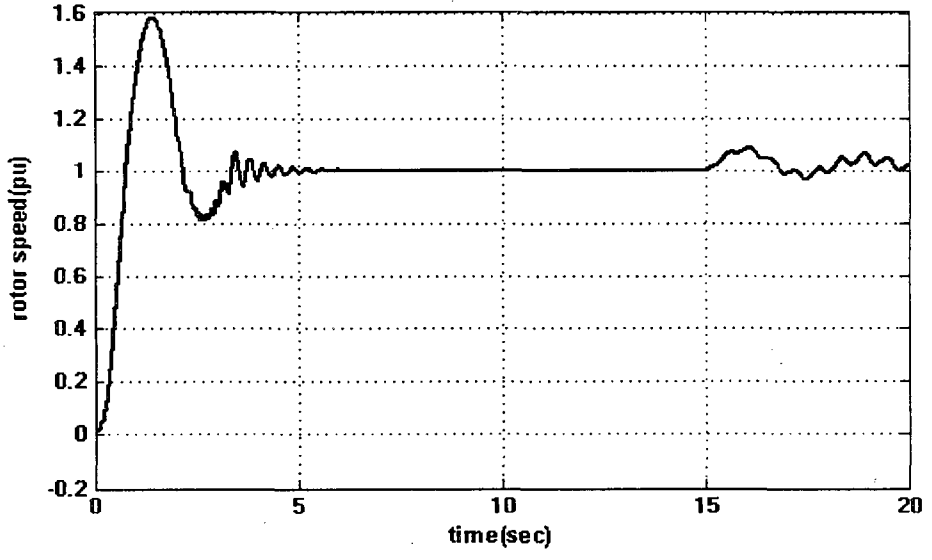

(b) Rotor speed (pu) with 75% of rated load and load Q_f=1.8

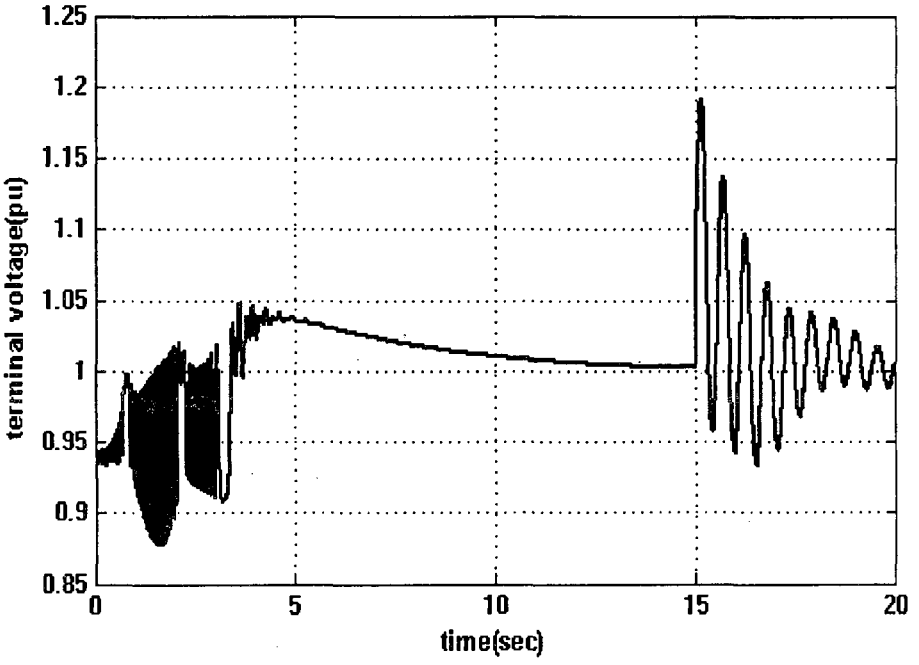

(c) Terminal voltage (pu) with 100% of rated load and load Q_f=1.8

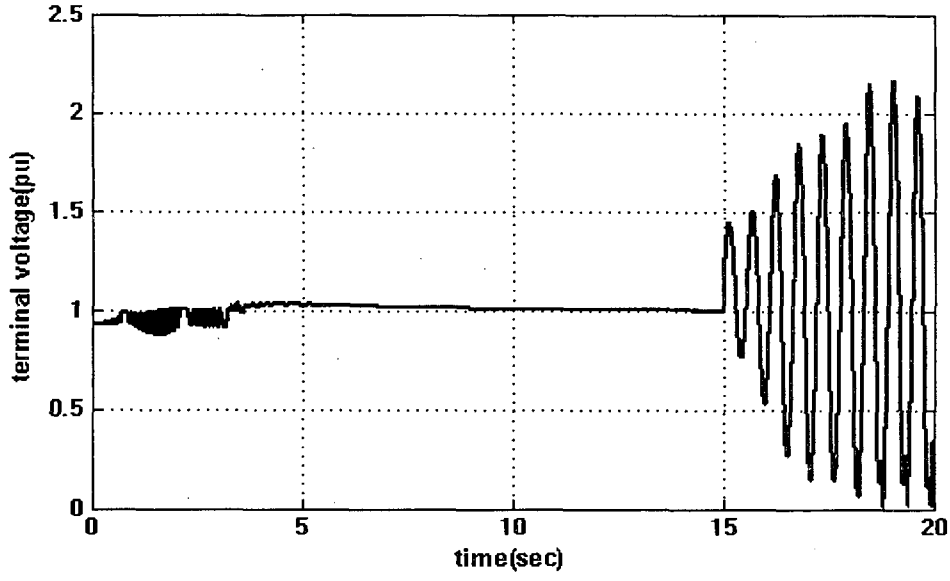

(d) Terminal voltage (pu) with 75% of rated load and load Q_f=1.8

Figure 4.10 Simulation results with RLC load (islanding occurs at t=15 seconds)

It can also be seen that after islanding the terminal voltage oscillate away quickly. The changes in frequency/rotor speed are caused by the fluctuating active power of the load when the terminal voltage is varying due to the addition of the AI schemes. In this case, the detection of the islanding can be triggered by either under/over frequency or an under/over voltage relay.

4.5.4 Performance Evaluation with Motor Load

As indicated in the previous section, motors form a major portion of system loads. Hence, it is important to investigate the motor load impact on the islanding protection. In this thesis, an induction motor model in MATLAB is used to represent a general population of motors ranging in types from those in small residential/industrial applications to large motors. Studies [15] show that the most important sensitivity

influencing the system dynamics is the percentage of motors at the load bus. Variations in the motor inertia and impedances are not as great an influence on the system dynamics as the percentage of motors. Here, the extreme case with 100% penetration of induction motor load (Power Rating=150 kVA) is simulated to evaluate its impact on the performance of the AI schemes. In the simulation, a capacitor is connected in parallel to the motor so as to compensate the reactive power of the induction motor.

The same conditions have been simulated. Compared with the previous simulation results for RLC load, the active power AI scheme for the induction motor is not as effective as for the RLC load. In this case, actually, it responds slowly to detect the islanding within a 2-second time window because the rotor speed is still within the normal range.

On the other hand, the voltage magnitude oscillates dramatically due to the reactive power AI scheme. The islanding can be easily detected by an over-voltage relay. It is concluded that the reactive power scheme is more effective for motor load than the active power scheme. This is consistent with the frequency-domain analysis.

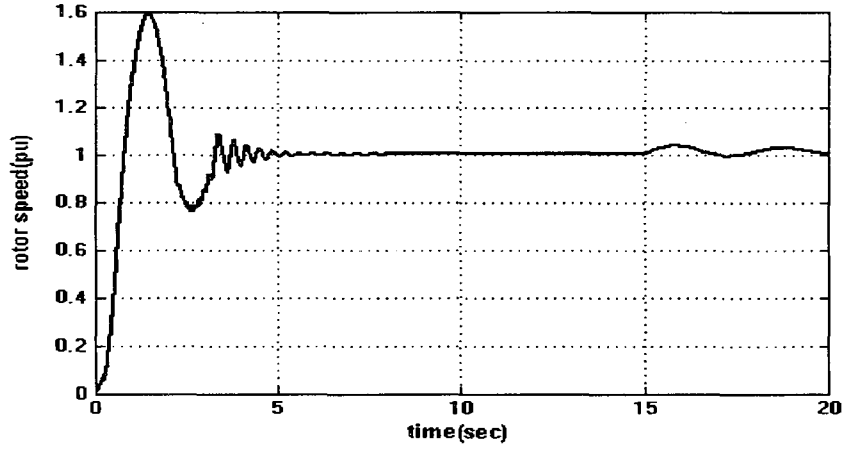

(a) Rotor speed (pu) with100% rated load and $0.8p_f$

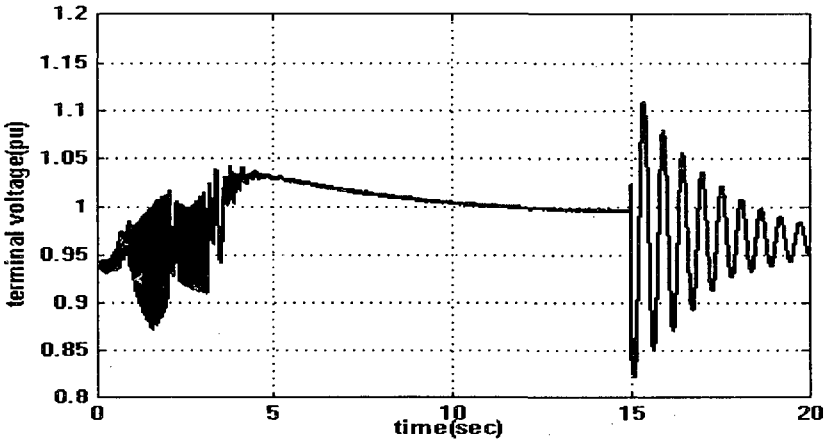

(b) Terminal voltage (pu) with 100% rated load and $0.8p_f$

Figure 4.11 Simulation results with Motor load (islanding occurs at t=15 seconds)

In all the different loading conditions, the reactive power AI scheme is stronger than the active power scheme in responding to unintentional islanding.

4.5.5 Generator Response to Three-Phase Fault

A three-phase fault is applied at the high-voltage side of the distribution transformer at t=15s and lasts about 5 seconds. The responses of the frequency and voltage from the simulations are shown in Figure 4.10.

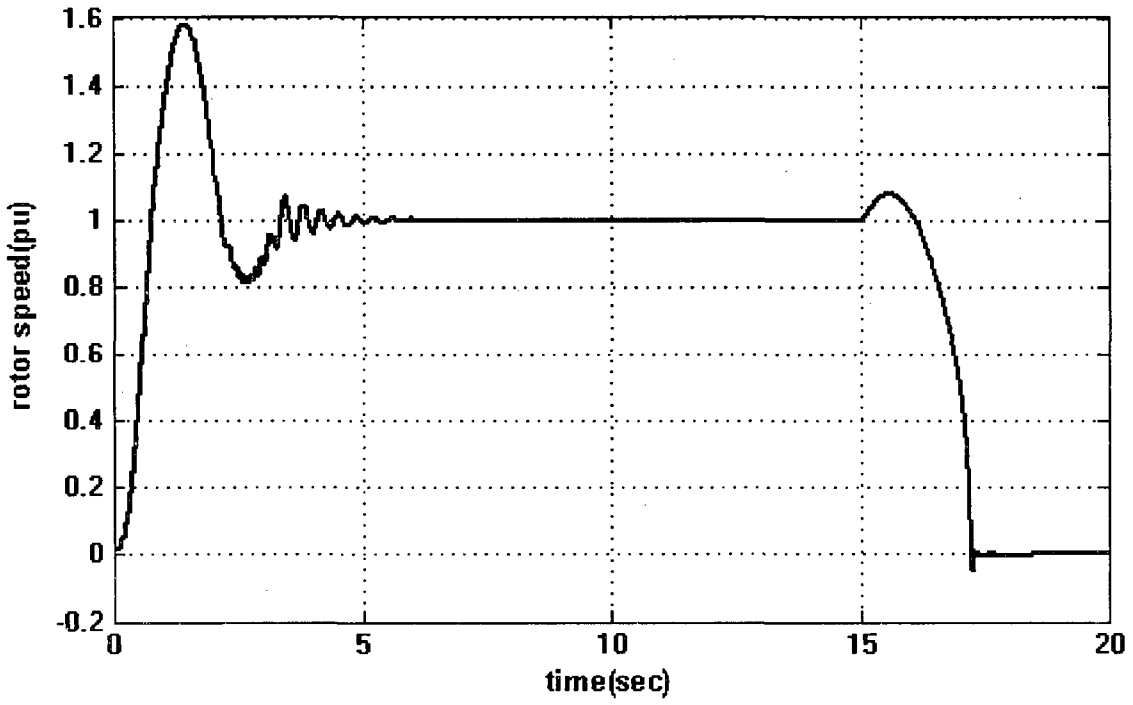

(a) Rotor speed (pu)

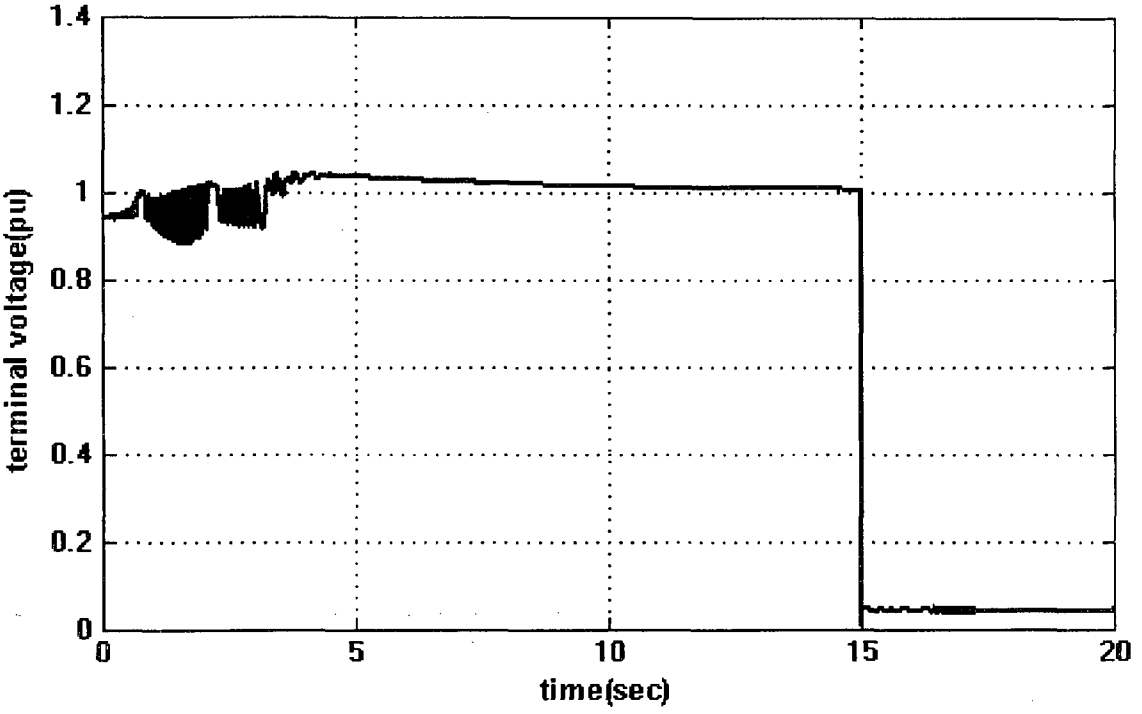

(b) Terminal voltage (pu)

Figure 4.12 Simulation results of the response to a three-phase fault

When a fault happens, the AI schemes have a very fast and strong response to drift away from the normal operating range of voltage and frequency.

CHAPTER 5

CONCLUSIONS

In this thesis, an anti-islanding (AI) scheme: namely the active power AI scheme and the reactive power AI scheme for synchronous machine-based distributed generations is analyzed. These DGs include engine generators (diesel, natural gas, biomass, hydrogen) and gas turbines. In the thesis, the detailed discussions and simulation studies, including theoretical analysis and the design guidelines for the new AI schemes and computer simulations, have been covered.

The positive feedback created by the active/reactive power AI compensator will drive the frequency/voltage to be out of the normal ranges once the DG is islanded. One of the outstanding features is that the proposed schemes can show discrimination between actual islanding and other non-islanding disturbances. This is very hard for any passive scheme to achieve. Since the new schemes are designed as part of the DG control, the cost to implement the schemes is basically negligible.

In the first part of this thesis, the characteristics and modeling of the power system using Park's transformation was covered in considerable detail. After that, the positive feedback concept with the principles of the applications was introduced. With the frequency-domain analysis in MATLAB, the effectiveness of the new active/reactive power AI schemes has been evaluated over a wide range of load conditions. The study

concludes that the reactive power AI scheme is more effective than the active power AI scheme. The illustrative time-domain simulations conducted in MATLAB have validated the frequency-domain analysis conducted in MATLAB.

Hence, it is possible to suggest the following findings:

- The reactive power AI scheme is very effective for every kind of load. It responds quickly, i.e. detecting islanding within 2.0s, by drifting away from the nominal value even when the power is closely matched between the generation and the load.
- It can detect islanding at different power levels. But if there is a power mismatch, the response will be magnified.
- For different quality factors, Qf, the response is sufficient. It responds as effective with a high Qf load as with a low Qf load.
- The reactive power AI scheme is superior to the active power AI scheme due to its high effectiveness for a high penetration of motor loads. However, the nominal operation of the DG equipped with the reactive power AI scheme can be affected more adversely by the grid impedance and voltage disturbances.

In summary, the positive feedback AI schemes are highly effective when compared with other AI schemes and easy to implement.

APPENDIX

MACHINE PARAMETERS

A.1 Synchronous Machine Data

The data for the generator used in the simulation studies is obtained from [8].

Machine rating: 150 kW.

Machine rated voltage (line-to-line RMS): 480V.

Inertia Constant: H =2.00 MW/MVA

Machine Reactance values (in pu):

Xd=10.823 pu; Xq=5.325 pu; X'd=0.863 pu; X''d= 0.258 pu; X''q=0.304 pu;

Time constant value (in pu):

T'd0=2.11s; T"d0=0.0227s; T"q0=0.176s; Xl=0.0892pu; Ra=0.022pu.

Load Parameters (100 % of Load):

R=1.536 ohms

L=2.26354 [mH]

C=3.108295 [mF]

For the system with voltage and frequency control

Exciter Data:

K_1=0.0625 pu; T_1=100 pu;

K_2=33 pu; K_2=0.02 sec;

K_3=1.0 pu; K_2=0.0159 sec.

Governor Data:

T_G=1.0 sec;

R_G=5% pu.

A.2 Induction Motor Data

The data for the induction motor used in the simulation studies is obtained from [9].

Stator winding resistance R_a= 0.0068 pu;

Stator leakage inductance L_l= 0.1 pu;

Magnetizing inductance L_m= 3.4 pu;

Synchronous inductance L_s= 3.5 pu;

Rotor resistance R_2=0.018 pu;

Rotor leakage inductance L_2=0.07 pu;

Inertia constant H=0.5 MW/MVA

Load model exponent D=2 pu;

BIBLOGRAPHY

[1] IEEE Standard for Interconnecting Distributed Resources with Electric Power Systems, IEEE, Standards Coordinating Committee 21, July 2003.

[2] R.M.Rifaat, Critical Considerations for Utility/Cogeneration Inter-Tie Protection Scheme Configuration", IEEE Transactions on Industry Applications, Vol. 31, N 5, September/October 1995. pp 973 – 977.

[3] W. Bower and M. Ropp, Evaluation of Islanding Detection Methods For Photovoltaic Utility, International Energy Agency, Report IEA PVPS T5-09: 2002.

[4] P. C. Krause, Analysis of Electric Machinery, New York: McGraw Hill, Inc., 1987.

[5] IEEE recommended practices for excitation System Models for Power System Stability Studies, IEEE STD 421.5-1992, and Aug. 1992.

[6] W. B. Gish, W. E. Feero, and S. Greuel, Ferro resonance and loading relationships for DSG installations, IEEE Trans. Power Del., vol. PWRD-2, no. 3, pp. 953–959, Jul. 1987.

[7] C. L. Wagner, W. E. Feero, W. B. Gish, and R. H. Jones, Relay performance in DSG islands, IEEE Trans. Power Del., vol. 4, no. 1, pp. 122–131, Jan. 1989.

[8] Jadric, I.; Boroyevich, D.; Jadric, M. Modeling and Control of a Synchronous Generator with an Active DC Load, IEEE transactions on Power Electronics, Vol. 15 No.2, pp.303 – 311, March 2000.

[9] Pereira, L.; Kosterev, D.; Mackin, P.; Davies, D.; Undrill, J.; Zhu, W., An interim dynamic induction motor model for stability studies in WSCC, IEEE Transactions on Power Systems, Vol.17, No. 4, pp.1108-1115, November 2002.

[10] Wen-Jung Chiang; Hurng-Lahng Jou and et al, Novel Active Islanding Detection Method for Distributed Power Generation System, International Conference on power Systems Technology, 2006.

[11] P. Du; J.K Nelson and Z. Ye; Active anti-islanding Schemes for Synchronous Machine based Distributed Generators, IEEE transactions on generation, Vol. 152, No. 5, September 2005.

[12] Jan Machowski; Janusz W. Bialek; James R. Bumby, Power System Dynamics and Stability, England; John Wiley & Sons, 1997.

[13] Fabio Saccomanno; Electric Power Systems, IEEE Press Series; New Jersey; John Wiley & Sons, 2003.

[14] Stefani, Savant, Shahian, Hostetter; Design of Feedback Control Systems, Orlando; Saunders College Publishing; 1994.

[15] Stanley M. Shinners; Modern Control System Theory and Design, 2nd Edition; New York; John Wiley & Sons; 1998.

VITA

Graduate College
University of Nevada, Las Vegas

Temesgen B. Tadegegn

Home Address:

5711 W. Tropicana Ave. Apt. # 318
Las Vegas, NV 89103
USA

Degrees:

Associate Degree in Business Administration
Ethiopian Adventist College

Bachelor of Technology
Defense University of Ethiopia

Special Honor and Awards:

Honor Graduate of Ethiopian Adventist College
Honor Graduate of Defense University of Ethiopia
Alliance of Professionals of African Heritage

Thesis Title:

Anti-islanding Schemes for Machine based Distributed Generation

Thesis Examination Committee:

Chairperson: Yahia Bahgzouz, Ph.D
Committee Member: Emma Regentova, Ph.D
Committee Member: Venkatesan Muthukumar, Ph.D
Graduate College Reperesentative: Robert Boehm, Ph.D